The influence of neuronal calcium sensor 1 on metastasis of triple-negative breast cancer

Inaugural-Dissertation

zur Erlangung des Doktorgrades

der Hohen Medizinischen Fakultät

der Rheinischen Friedrich-Wilhelms-Universität

Bonn

Jonathan Edem Apasu

aus Caserta / Italien

2020

Angefertigt mit der Genehmigung

der Medizinischen Fakultät der Universität Bonn

1. Gutachter: PD Dr. rer. nat. Ronald Jabs
2. Gutachter: Prof. Dr. rer. nat. Stephan Baader

Tag der Mündlichen Prüfung: 30.09.2020

Aus dem Institut für Zelluläre Neurowissenschaften

Direktor: Prof. Dr. rer. nat. Christian Steinhäuser

Table of Contents

List of Abbreviations

2/3-D	2/3-dimensional
ER	endoplasmic reticulum
GFP	green fluorescent protein
H&E	hematoxylin and eosin
InsP3R	inositol 1,4,5-trisphosphate receptor
LIMK1	LIM domain kinase 1
MSD	mean squared displacement
NCS1	neuronal calcium sensor 1
NFκB	nuclear factor kappa-light-chain-enhancer of activated B cells
PI3K / AKT	phosphatidylinositol 3-kinase – AKT protein kinase
PI4K	phosphatidylinositol 4-OH kinase

1. Summary

1.1 Introduction

Presently, breast cancer is the deadliest cancer in women worldwide and among the foremost reasons for morbidity and mortality in females overall (Becker, 2015). In most cases, cancer patients do not succumb to the primary tumor, but rather to its metastatic spread to distant organs (Mehlen and Puisieux, 2006). The most common sites of breast cancer metastasis are lungs and bones (Lee, 1985).

The capacity to spread to distant organs constitutes a hallmark of aggressive cancers and belongs to the defining characteristics which ultimately distinguish a malignant cancer from a benign tumor (Hanahan and Weinberg, 2011). This metastatic demeanor is enabled by certain crucial features (Lambert et al., 2017). Among these critical features are the ability of cancer cells to invade into the bloodstream, survival of the cells in the bloodstream, extravasation at the site of distant metastasis, and survival and growth in the secondary organ (Lambert et al., 2017).

The standard treatment for local, non-metastatic breast cancer are surgery and local radiation (Fisher et al., 2002). Yet, in cases of metastatic disease, systemic pharmaceutical treatment of particular cancer properties becomes most relevant (Waks and Winer, 2019). Nowadays, progesterone receptor-, estrogen receptor- or human epidermal growth factor 2- positive breast cancers can be targeted over their specific molecular markers (Waks and Winer, 2019). Nevertheless, triple-negative breast cancer - defined by the absence of these molecular markers - is not susceptible to the aforementioned targeted therapies, even though triple-negative breast cancer represents the most aggressive subtype with the poorest survival rate (Hudis and Gianni, 2011). Therefore, there is an urgent need to discover and evaluate new prognostic and therapeutic markers for triple-negative breast cancer.

A recently reported retrospective study of two independent breast cancer patient cohorts demonstrated that neuronal calcium sensor 1 (NCS1) reduced long-term survival and promoted distant metastasis in women suffering from breast cancer, regardless of the

estrogen receptor, progesterone receptor, and human epidermal growth factor 2 status (Moore et al., 2017). Another study, investigating the outcomes of patients suffering from liver cancer, demonstrated poor outcomes in patients with high NCS1 levels, underlining the relevance of NCS1 as a negative prognostic marker in cancer (Schuette et al., 2018).

NCS1 is a calcium binding protein, that is expressed at high levels in neurons (Schaad et al., 1996). It consists of a N-terminal myristoylation site and four helix-loop-helix EF-hand domains, out of which three bind calcium (Boeckel and Ehrlich, 2018). As NCS1 has been identified in non-neuronal tissue, it is acknowledged that it also has relevant functions outside of neurons (Blasiole et al., 2005; Gromada et al., 2005; Weiss et al., 2000).

NCS1 interacts with a variety of proteins, including the inositol 1,4,5-trisphosphate receptor (InsP3R) and the phosphatidylinositol 4-OH kinase (PI4K) (Haynes et al., 2006; Rajebhosale et al., 2003; Schlecker et al., 2006). These protein–protein interactions regulate central cellular processes like exocytosis, cellular survival and the InsP3R signaling pathway (Boehmerle et al., 2006; Choe and Ehrlich, 2006; Koizumi et al., 2002; Nguyen et al. 2019). NCS1 has been previously described as a survival factor through the indirect activation of the phosphatidylinositol 3-kinase – AKT protein kinase (PI3K / AKT) pathway (Nakamura et al., 2006). Interestingly, the PI3K / AKT pathway is often altered in cancer (Vivanco and Sawyers, 2002). Additionally, increased NCS1 levels have been described to promote intracellular calcium signaling (Nguyen et al., 2019; Schlecker et al., 2006). Calcium is a central second messenger ion, which enters the cytoplasm from the extracellular space and from intracellular storages, like the endoplasmic reticulum (ER) and mitochondria, through voltage-, or ligand-gated channels (Berridge, 1993, 1998; Gunter and Pfeiffer, 1990; Nguyen et al., 1998).

Crucial cellular processes such as cell growth and proliferation, cell cycle progression, apoptotic cell death and cell motility are regulated by alterations in the intracellular calcium concentration (Clapham, 2007; Hajnoczky et al., 2003; Zheng and Poo, 2007). Accordingly, perturbed calcium signaling has been associated with aggressive, highly metastatic cancers (Ando et al., 2018; Prevarskaya et al., 2011; Stewart et al., 2015). Thus, calcium binding molecules that mediate its downstream effects might function as potential biomarkers and therapeutic targets in cancer.

Recent investigations have revealed the relevance of NCS1 in promoting metastatic hallmarks in vitro, by demonstrating altered adhesive and invasive capabilities of two distinct breast cancer cell lines due to NCS1 overexpression (Moore et al., 2017). Additionally, NCS1 has been reported to promote cell survival of human breast cancer cells (Nguyen et al., 2019). In combination with the aforementioned physiologic roles of calcium and NCS1, these reported findings, strongly suggest that high NCS1 could have a metastasis promoting and outcome compromising effect on cancer cells. Consequently, it was hypothesized that NCS1 promotes metastatic spread of triple-negative breast cancer in vivo (Apasu et al., 2019). It is hoped that NCS1 will qualify as a predictive biomarker for cancer progression in general and for triple-negative breast cancer, in particular.

This hypothesis was tested by utilizing a previously developed mouse xenograft model to mimic lung metastasis of breast cancer (Fantozzi and Christofori, 2006). In combination with a luciferase, photon-flux based, live imaging system, this model allowed the observation of lung metastasis formation in xenografted mice over the course of 4 weeks. Moreover, within the same study, histopathologic evaluation of harvested mouse lungs was performed to evaluate possible pro-metastatic effects of NCS1 in the xenografted mice. The amount of vital metastasized breast cancer cells at early timepoints, as well as the extend of necrosis in the formed metastases in late timepoints of the study, were assessed.

Furthermore, in an attempt to explain the mechanics behind the enhanced metastatic capability, the effect of NCS1 on cell proliferation, cell morphology, the localization of NCS1 within the cell, as well as the role of NCS1 in cell migration in 2- dimensional (2-D) and 3-dimensional (3-D) assays, were investigated.

1.2 Hypothesis

It was hypothesized that NCS1 promotes lung metastasis of triple negative breast cancer. Consequently, elevated NCS1 levels were hypothesized to significantly increase metastatic capabilities in both in vitro assays and in a mouse xenograft model designed to evaluate lung metastasis of triple negative breast cancer cells.

1.3 Material and Methods

1.3.1 Cell culture

A stable NCS1 overexpressing MDA-MB 231 cell line and a concurrently made control cell line, used for the in vitro and in vivo experiments, were generated and maintained as described previously (Apasu et al., 2019; Moore et al., 2017).

1.3.2 Cell proliferation assays

Two distinct cell proliferation assays, the CellTiter-Glo assay (Promega, Madison, Wisconsin, USA) and the AlamarBlue assay (Thermo Fisher Scientific, Waltham, Massachusetts, USA), were performed to evaluate the influence of NCS1 on the proliferation rates of the created MDA-MB 231 cell lines (Apasu et al., 2019).

1.3.3 Scratch assay and colony formation assay

A scratch assay and a colony formation assay were performed with the NCS1 overexpressing and NCS1 control MDA-MB 231 cells to investigate the influence of NCS1 on motility and cell survival in a 2-D environment (Apasu et al., 2019).

1.3.4 Assessment of NCS1 mRNA and NCS1 protein levels

To investigate the increased expression levels of NCS1 mRNA in the NCS1 overexpressing cells as compared to the NCS1 control cells, a quantitative RT-PCR was performed and NCS1 mRNA expression fold changes were calculated, following the ΔΔCt method (Apasu et al., 2019; Livak and Schmittgen, 2001). Western blot was performed to verify the successful increase in NCS1 protein levels (Apasu et al., 2019).

1.3.5 Immunofluorescence microscopy

To investigate the localization of NCS1 within the cells, NCS1 overexpressing and control MDA-MB 231 cells were plated on cover slips, fixated and antibody labeled before being examined with a confocal microscope (Apasu et al., 2019).

1.3.6 Transduction of cells with the bioluminescence reporter

To enable bioluminescent imaging of the engineered NCS1 overexpressing or control MDA-MB 231 cells, they were retrovirally infected with a previously characterized triple-fusion protein reporter (Ponomarev et al., 2004). This reporter encodes for the herpes simplex virus thymidine kinase 1, green fluorescent protein (GFP) and firefly luciferase. Using the Clontech Calcium Phosphate Transfection Kit (Clontech Laboratories, Mountain View, California, USA) and a polybrene facilitated infection, the cells were equipped with the reporter. Successfully transduced cells were selected via cell-sorting for GFP positivity with a high-speed cell sorter (Apasu et al., 2019). The Promega Luciferase Assay System (Promega, Madison, Wisconsin, USA) was utilized to verify a sufficient expression of luciferase in the transduced MDA-MB 231 cells (Apasu et al., 2019).

1.3.7 Embedding MDA-MB 231 cancer cells in a 3-D collagen I matrix and analysis of cell shape, velocity, and mean squared displacement (MSD)

To evaluate cell shape, velocity, and MSD of NCS1 overexpressing and NCS1 control MDA-MB 231 cells in a 3-D environment, the cells were embedded in a 3-D collagen I matrix (Apasu et al., 2019). A confocal microscope was used for cell imaging, ImageJ (National Institutes of Health, Bethesda, Maryland, USA) was used to manually track cell migration, custom scripts in MatLab (MathWorks, Natick, Massachusetts, USA) were utilized to analyze the resulting output before finally calculating average speed and MSD (Apasu et al., 2019).

1.3.8 Approval of animal studies

All mouse work was approved by the Yale University Institutional Animal Care & Use Committee.

1.3.9 Tail vein injection

7-9 weeks old, female, athymic Balb/c nude mice, were utilized for the xenografting study. Athymic Balb/c nude mice lack an intact cellular immune system (Pelleitier and Montplaisir, 1975). Hence, injected cancer cells from a different organism do not evoke an immune response and can grow in a xenografted mouse. NCS1 control or NCS1 overexpressing MDA-MB 231 cells, respectively, were injected into the lateral tail vein of the mice. Subsequently, mice were imaged as described in the following and unsuccessfully xenografted mice were excluded from the study (Apasu et al., 2019).

1.3.10 Bioluminescent imaging

Mice were anesthetized, retro-orbitally injected with luciferin and imaged with a live imaging and analysis software (Apasu et al., 2019). Then, the photon-flux (in photons per second) from the xenografted MDA-MB 231 cells was measured within a region of interest over the mouse lung. This allowed the assessment of the tumor burden in the mouse lung, since the photon-flux is proportional to the number of light-emitting cancer cells (Lim et al., 2009). In the course of the study, all photon-flux values were normalized to the photon-flux values obtained immediately after xenografting, and in this manner all mice started with a relative bioluminescence signal of 1 (Apasu et al., 2019).

1.3.11 Harvest and histopathologic analysis of mouse lungs

On day 3 and day 7 post xenografting, as well as at the end of the study, the lungs were collected for histopathologic evaluation (Apasu et al., 2019). Hematoxylin and eosin (H&E) stained slides were created and NSC1 presence was confirmed by anti-NCS1

immunohistochemical staining, according to a previously described protocol (Moore et al., 2017). All slides were blindly evaluated by an experience pathologist.

1.3.12 Statistical analysis

All final analyses were done using the Python programming language (v.3.6; https://www.python.org/), unless stated otherwise. To compare the mean values of 2 independent datasets, an independent 2-sample Student's t test was performed; values of $p < 0.05$ were considered significant. Whenever possible, error bars were plotted indicating either 95 % confidence intervals or the +/- standard error of the mean (Apasu et al., 2019).

1.4 Results

1.4.1 Engineered MDA-MB 231 cells stably overexpress NCS1

In order to evaluate the function of NCS1 in vitro and in vivo, stably NCS1 overexpressing MDA-MB 231 breast cancer cells, as well as control cells, were generated (Moore et al., 2017). The successful overexpression of NCS1 was confirmed by immunoblot (Fig. 1A; Apasu et al., 2019). On average, NCS1 mRNA expression levels were 4-fold higher in NCS1 overexpressing cells when compared to NCS1 control cells, as confirmed by real-time quantitative PCR measurements. Normalization to the housekeeping genes ACTB and S18 yielded identical results.

1.4.2 NCS1 does not influence cell proliferation rate

To investigate if NCS1 overexpression confers an aggressive tumor phenotype by promoting proliferation, an ATP- based growth assay was utilized to measure cell growth of NCS1 overexpressing and control cells over a period of 5 days. No difference in the proliferation rates of the cell lines was observed (Fig. 1B; Apasu et al., 2019). This is in line with previously reported results (Moore et al., 2017). To confirm these

results, the proliferation rates of NCS1 overexpressing MDA-MB 231 cells and control MDA-MB 231 cells were compared with an AlamarBlue assay. Again, the proliferation rates were similar.

1.4.3 NCS1 reduces cell circularity and increases cellular protrusions

NCS1 overexpressing cells showed distinct cell morphology in a 3-D environment (Fig. 1C; Apasu et al., 2019). In particular, NCS1 overexpressing cells were significantly less circular and had a higher aspect ratio compared to the control (Fig. 1D; Apasu et al., 2019). Large cellular protrusions were only seen in the NCS1 overexpressing group.

1.4.4 NCS1 localizes to cellular protrusions and colocalizes with actin at the leading edge

Immunofluorescence microscopy revealed that, regardless of total NCS1 levels, NCS1 preferentially localizes at cellular protrusions within the cell, including the lamellipodia (Fig. 2A, Fig. 2B; Apasu et al., 2019). Further, NCS1 was seen to extensively colocalize with actin at the leading edge, but not with stress fibers or cytoplasmic actin puncta.

1.4.5 Colony formation is promoted by NCS1 overexpression

A colony formation assay was performed to test if NCS1 facilitates tumor growth and metastasis by increasing cell survival and motility. After plating and maintaining cells in a cell culture dish for 14 days, the resulting colonies were fixed and stained. Subsequently, the total area covered by the cells was calculated. Regardless of the number of initially planted cells, the ability to form colonies was significantly increased in NCS1 overexpressing cells, as compared to NCS1 control cells (Fig. 3A; Apasu et al., 2019). High NCS1 therefore promotes colony formation of MDA-MB 231 breast cancer cells.

1.4.6 NCS1 promotes cell motility in 2-D and 3-D assays

2-D motility was assessed by placing cells in a cell culture dish and applying a standardized scratch-wound after the formation of a cell monolayer. Subsequently, the relative traveled distance of NCS1 overexpressing and NCS1 control cells was measured after 24 h, as a metric for the wound closure ability of the cells. The scratched area in the monolayer was significantly more closed by NCS1 overexpressing cells than by the control cells (Fig. 3B; Apasu et al., 2019). This suggests that 2-D migration was increased by NCS1 overexpression. Thereafter, NCS1 overexpressing and control cells were placed in a collagen matrix and time-lapse microscopy captured the cell movement over time, to validate the results within a 3-D migration assay. Although the movement was not directional regardless of NCS1 levels, considerably more movement was observed in the NCS1 overexpressing condition (Fig. 3C; Apasu et al., 2019). After 8 h MSD was increased in NCS1 overexpressing cells (Fig. 3D; Apasu et al., 2019). Additionally, average cell velocity was significantly higher in NCS1 overexpressing cells than in the control cells (Fig. 3E; Apasu et al., 2019). In sum, as shown in 2-D assays, NCS1 promoted migration in a 3-D collagen gel.

1.4.7 NCS1 overexpression promotes lung metastasis of MDA-MB 231 cells

The effects of NCS1 overexpression were explored in a mouse model of breast cancer metastasis (Fantozzi and Christofori, 2006). MDA-MB 231 cells, with either NCS1 overexpression or NCS1 control levels, were transduced with a firefly luciferase reporter to enable live imaging. Subsequently, the cells were injected in the lateral tail vein of female athymic nude mice, causing the bloodstream to transport the cells into the lungs. The tumor burden in the mouse lungs was quantified by measuring the photon-flux after luciferin injection. Photon-flux was measured in lung imaging studies on day 0, 1, 3, 7, 14, 21, and 28 after xenografting (Fig. 4A; Apasu et al., 2019). As expected, the majority of cells were observed in the lungs and no luminescence signal was found in other organs. Comparison of the tumor burden amongst individual mice was enabled by normalizing the total flux of each day to the total flux on day 0 of the measured mouse. Interestingly, the

outcome limiting effects of NCS1 overexpression were observed between day 0 and day 7. This was reflected by a yield of higher relative photon-flux in the group injected with NCS1 overexpressing cells. In this timeframe NCS1 overexpression appears to promote a survival advantage of the injected cells, which suggests that NCS1 overexpressing tumor cells have a survival advantage in the early phase of metastasis formation and is in line with previously reported in vitro findings (Moore et al., 2017; Nguyen et al., 2019). In agreement with the observed unchanged proliferation rates in the in vitro setting (Fig. 1B; Apasu et al., 2019), the tumor growth rates from day 7 onwards were similar in the NCS1 overexpressing and the NCS1 control group, as reflected by the parallel curves from day 7 onwards (Fig. 4C; Apasu et al., 2019).

1.4.8 Lung histology confirms higher tumor burden in mice xenografted with NCS1 overexpressing cells

Mouse lungs were harvested at day 3 and day 7, as well as at the end of the aforementioned xenografting study (Fig. 4A; Apasu et al., 2019). Based on in vitro studies and the results of the in vivo imaging, the biggest differences between NCS1 overexpressing and NCS1 control groups were expected in the early phase (defined as the first 7 days) of tumor development. Therefore, histopathologic assessment of the lung tissue was focused on these early time points. Only scarce cancer cells were found in the H&E stained lung specimens collected from the NCS1 control mice (Fig. 5A; Apasu et al., 2019). A few single cancer cells were found in only 3 out of 8 NCS1 control mouse lungs. In contrast to this finding, cancer cells were detected in all 8 collected lungs from mice xenografted with NCS1 overexpressing MDA-MB 231 cells. In addition, 6 out of these 8 lungs demonstrated multiple tumor cell clusters (Fig. 5B, Fig. 5C; Apasu et al., 2019). To validate the expression of NCS1 in the identified cancer cells, the H&E-stained slides were stained with anti-NCS1 immunohistochemistry (Fig. 5C; Apasu et al., 2019). The results of the histopathologic assessment validate the results of the photon-flux study, indicating that NCS1 overexpression causes increased early incidence of metastasis in mouse lungs after tail-vein injection of breast cancer cells. Both the increased invasive capabilities and the promotion of tumor cell survival by NCS1 overexpression can explain this observation.

1.4.9 NCS1 protects cancer cells from necrosis within mature tumors

To explore the function of NCS1 in mature tumors, mouse lungs were collected at the endpoint of the xenografting study and H&E stained for their histopathological investigation. The endpoint of the xenografting study was defined by the absolute photon-flux, measured over the mouse lung, surpassing the threshold of 10^9 photons per second. This photon-flux threshold was reflective of the tumor burden in the lung reaching a large, predetermined size. As the lungs were completely filled with tumor cells at this point of the study in both conditions, as expected, no difference in regard to the overall tumor volume was observed between NCS1 overexpressing and control lungs. Likewise, a similar histologic appearance of the lung metastases formed by the injected NCS1 overexpressing and NCS1 control cells was anticipated. In contrast to this anticipation, the control tumors exhibited vast areas of necrosis (Fig. 6A; Apasu et al., 2019), whereas 3 out of 4 lung metastasis specimens from mice, xenografted with NCS1 overexpressing cells, showed no necrotic cells (Fig. 6B; Apasu et al., 2019). In only one specimen of the NCS1 overexpressing lung metastases, scarce amounts of necrotic material could be detected, as opposed to the profound prevalence of necrosis in the NCS1 control lung metastases. This finding not only indicates that NCS1 provides a survival advantage for single tumor cells in the blood flow and in the beginning of metastasis, it also indicates that NCS1 promotes tumor cell survival in mature tumors.

1.5 Discussion

Metastasis is a multistep process that involves the detachment of cancer cells from the primary tumor, the intravasation of the cells into the blood vessels, the survival of the cells in the blood circulation, the extravasation at the site of metastasis and finally, survival and growth in the distant organ (Fidler, 2003; Gupta and Massagué, 2006). Circulating tumor cells can be detected in the blood of cancer patients without manifest metastases (Mehlen and Puisieux, 2006; Pantel and Brakenhoff, 2004). This implies that the detachment from the primary tumor and the intravasation of the cancer cells into the bloodstream are indicators, but rather the aforementioned steps that follow the intravasation are most crucial in cancer metastasis. It was consequently decided to test the hypothesis, that

NCS1 promotes lung metastasis of triple-negative breast cancer, in a mouse xenograft model that directly simulates a situation in which there are circulating cancer cells in the bloodstream (Fantozzi and Christofori, 2006).

The aim of this dissertation was to evaluate the influence of NCS1 on the metastasis of triple-negative breast cancer and to discuss possible mechanistic pathways, by which NCS1 might confer a pro-metastatic phenotype.

High NCS1 levels have been linked to negative outcomes in breast cancer patients as well as in patients suffering from liver cancer (Bong et al., 2020; Moore et al., 2017; Schuette et al., 2018). NCS1 has also been described to alter crucial pro-metastatic capabilities, including invasion and adhesion, in the breast cancer cell lines MDA-MB 231 and MCF-7 (Grosshans et al., 2020; Moore et al., 2017).

With the final intention to investigate the role of NCS1 in a mouse xenograft model of triple-negative breast cancer metastasis, NCS1 was first stably overexpressed in the triple-negative MDA-MB 231 breast cancer cell line. The original MDA-MB 231 cells were obtained from the pleural effusion of a breast cancer patient, suffering from distant metastasis (Cailleau et al., 1978). The intrinsic metastatic capability of these cells made them appropriate for a metastasis study.

Following the injection of these human, triple-negative breast cancer cells into the lateral tail vein of the mouse, the bloodstream transported the injected tumor cells to the lungs, where metastases were formed. In this study, assessment of lung metastasis was the focus, because the lung is one of the most common metastatic sites of breast cancer and NCS1 was reported to specifically promote lung metastasis in breast cancer patients (Lee, 1985; Moore et al., 2017). Accordingly, the capabilities of the injected cells to survive in the capillaries, to extravasate into the lung tissue and to survive in the lung microenvironment - which are important capabilities of metastasis formation - were sufficiently tested in the xenograft study (Lambert et al., 2017). Overall, the results indicate that NCS1 promoted lung metastasis by enhancing early metastasis into the lung and promoting cell survival within the formed metastases. It was demonstrated that mice, xenografted with the NCS1 overexpressing cells, developed lung metastases faster than

mice xenografted with NCS1 control cells. Another interesting observation was provided by the histopathologic assessment of the formed lung metastases. NCS1 overexpression protected the tumor cells from necrosis within the tumor, which implies effects of NCS1 that extend beyond the first phase of metastasis. NCS1 was hypothesized to promote tumor cell survival in mature tumors, as it promotes cell survival in vitro (Grosshans et al., 2020; Nguyen et al., 2019). In agreement with the in vitro findings, the tumor growth rate was not altered by NCS1. The pro-metastatic effect primarily occurred in the first 7 days after xenografting. This observation is in alignment with the results of other investigators, which demonstrated that NCS1 overexpression has no impact on cell proliferation but enhances invasive capabilities of NCS1 overexpressing breast cancer cell lines (Moore et al., 2017).

The study further provided robust evidence for altered cellular characteristics in NCS1 overexpressing cells, and these differences offer potential mechanistic explanations for how NCS1 promotes metastasis. After confirming unaltered proliferation rates by NCS1 overexpression, the effects of NCS1 overexpression on tumor cell morphology were investigated by immunofluorescence imaging (Moore et al., 2017). Herein, NCS1 overexpressing cells demonstrated altered cellular morphology. Compared to NCS1 control cells, the NCS1 overexpressing cells were less circular and had an increased amount of large cellular protrusions. This phenotype is related with increased cellular motility and invasion, which are both characteristics found in aggressive, metastatic tumors (Friedl and Gilmour, 2009; Gagliardi et al., 2015; Stuelten et al., 2018). Regardless of absolute NCS1 expression levels, NCS1 was concentrated in the leading edge of migrating cells, which would be expected to stimulate cancer cell migration by regulating local calcium at the cellular protrusions. The demonstrated colocalization between NCS1 and actin, specifically at the leading edge, suggests a role for NCS1 in assisting the regulation of the constant actin cytoskeleton turnover - a crucial mechanism for cancer cell migration (Yamaguchi and Condeelis, 2007).

To investigate a functional impact of NCS1 overexpression, 2-D colony formation and wound healing assays were performed. NCS1 overexpressing cells showed increased motility, compared to NCS1 control cells. To closer mimic the physiologic 3-D microenvironment in which cancer cells grow, NCS1 overexpressing cells and control cells

were placed in type I collagen gels. Subsequently, time-lapse microscopy of the MDA-MB 231 cells was performed. This allowed the investigation of cell movement dynamics in a 3-D microenvironment (Riching et al., 2014; Wu et al., 2014). As expected, the NCS1 overexpressing cells demonstrated increased motility, measured by MSD and average speed. In sum, these in vitro experiments imply that breast cancer cells, that obtain increased NCS1 levels in the course of tumorigenesis, gain increased motility. This, in turn, promotes their capability of forming distant metastases.

The exact role of NCS1 in cancer metastasis remains to be fully elucidated. However, when considering the role of NCS1 in calcium homeostasis, it is possible to present an initial understanding of how NCS1 confers a pro-metastatic phenotype. Intracellular calcium plays a central role in vital cellular processes like proliferation and growth of cells, apoptotic cell death and cell motility (Clapham, 2007; Hajnoczky et al., 2003; Zheng and Poo, 2007). During the latter for instance, the cyclic morphological and adherence changes that occur during cell migration are accompanied by certain calcium signaling patterns, like spikes or oscillations (Pettit and Fay, 1998). At present, it is acknowledged, that calcium regulates many major oncogenic pathways and accordingly, perturbed calcium signaling has been associated with aggressive, highly metastatic cancers (Prevarskaya et al., 2011; Stewart et al., 2015). Consequently, numerous calcium binding proteins that regulate downstream effects of calcium signals have been implicated in calcium dependent cancer progression, including S100 calcium binding proteins (Chen et al., 2013). S100A11 was reported to promote cancer aggressiveness through the upregulation of the PI3K / AKT signaling pathway (Xiao et al., 2018). The EF-hand calcium binding protein S100A4, has been shown to be relevant for calcium dependent metastatic pathways (Boye and Maelandsmo, 2010). Intriguingly, the calcium depended regulation of S100A4 results indirectly in increased migration (Tarabykina et al., 2007). NCS1, as well, is an EF-hand calcium binding protein (Boeckel and Ehrlich, 2018; Weiss et al., 2010).

NCS1 might promote metastatic capabilities and tumor progression through the PI3K / AKT pathway (Nakamura et al., 2006). This pathway is known to facilitate cell migration as well as increase cellular survival and phosphatidylinositol 3-kinases have been described to play a crucial role in cancer progression (Vivanco and Sawyers, 2002). NCS1

binds and activates the PI4K (Rajebhosale et al., 2003). The PI4K, in turn, catalyzes the production of phosphatidylinositol-messengers, which ultimately activate the PI3K / AKT pathway (Balla and Balla, 2006). A recent study reported increased AKT activity in NCS1 overexpressing triple negative breast cancer cells (Grosshans et al., 2020). Herein, it is demonstrated that NCS1 is upregulated by the stress-induced nuclear factor kappa-light-chain-enhancer of activated B cells (NFκB), subsequently promoting metastatic capabilities by activation of the PI3K / AKT pathway (Grosshans et al., 2020). Intriguingly, another novel publication demonstrated attenuated invasion and migration capabilities as well as decreased lung metastasis in a mouse model upon inhibition of the PI3K / AKT / NFκB pathway in triple negative breast cancer cells (Hseu et al., 2019). Additional recent studies confirm the relevance of the PI3K / AKT pathway in the pathophysiology of triple negative breast cancer by demonstrating decreased metastatic capabilities via inhibition of the pathway (Han et al., 2019; Zhang et al., 2019). These findings stress the potential therapeutic benefit of inhibiting the PI3K / AKT pathway in treatment of triple negative breast cancer by targeting NCS1.

NCS1 also directly interacts with the InsP3R at the ER, amplifying evoked calcium signals (Schlecker et al., 2006). A recent investigation has underlined the importance of the NCS1 - InsP3R interaction by demonstrating increased calcium signaling and cell survival by overexpression of NCS1 in a breast cancer cell line (Nguyen et al., 2019). In contrast to this, the overexpression of a NCS1-subtype, engineered to insufficiently bind InsP3R was unable to promote cell survival or calcium signaling. Conversely, another novel study demonstrated decreased cell survival and decreased inositol 1,4,5-trisphosphate-mediated calcium signaling by NCS1 knockout in triple negative breast cancer cells (Grosshans et al., 2020). These findings emphasize the relevance of the interaction between NCS1 and the InsP3R. InsP3Rs themselves also have been described to promote an aggressive, pro-metastatic phenotype in cancer cells (Ando et al., 2018).

Further, NCS1 has been closely associated with the expression of the LIM domain kinase 1 (LIMK1) (Schuette et al., 2018). The enzyme LIMK1 regulates cell motility by regulation of the actin cytoskeleton and its high expression has been correlated with increased invasive capabilities of cancer (Li et al., 2013; Scott et al., 2010; Scott and Olson, 2007). In order to invade the tumor surrounding tissue, cancer cells depend on increased levels

of LIMK1 (Scott et al., 2010). The inhibition of LIMK1, in turn, reduces their invasive capability (Li et al., 2013; Scott and Olson, 2007). Hence, the close association of NCS1 to LIMK1 expression offers another route through which NCS1 might render cancer cells more invasive.

In sum, NCS1 appears to promote tumor cell motility and tumor cell survival via multiple pathways. Various in vitro and in vivo experiments have demonstrated the effects of NCS1 overexpression on several aspects of the cellular phenotype. In depth mechanistic studies, to be performed in the future, will provide a better understanding of the exact mechanistic molecular effects of NCS1 on these pathways.

Triple-negative breast cancer remains a threat to women all over the world (Hudis and Gianni, 2011). However, NCS1 is a potential predictive biomarker to detect women with a more aggressive cancer who are at risk of suffering distant metastasis. This type of marker would allow physicians to start high-risk patients earlier on more potent therapeutic schemes in order to improve their disease related outcome.

Previously reported interactions of NCS1 with chemotherapeutic agents like paclitaxel, give hope for possible pharmaceutical NCS1-targeted therapy regimen (Boehmerle et al., 2006). Interestingly, a recently published study demonstrated that inhibition of NCS1 expression in triple negative breast cancer cells significantly promotes necrotic cell death induced by doxorubicin, a chemotherapeutic drug commonly used to treat triple negative breast cancer (Bong et al., 2020; Hudis and Gianni, 2011). Another novel publication revealed an attenuating effect of NSC1 knockout on the crucial pro-metastatic capabilities cell survival and migration (Grosshans et al., 2020). In addition, NCS1 has already been identified as a drug target in neurological disorders (Mo et al., 2012). This emphasizes that targeting of NCS1 in triple-negative breast cancer could, in fact, be a possible treatment option in future. Of additional clinical interest are other targets of the NCS1-associated calcium signaling complex, that might qualify for pharmacologic interventions to mitigate the effect of NCS1 on metastatic spread and cancer progression, not only in triple-negative breast cancer, but in cancer in general.

1.6 Summary

At present, breast cancer is the leading global cause of cancer morbidity and mortality in women. The most aggressive subtype - triple-negative breast cancer - evades current targeted therapy schemes and lacks sufficient prognostic markers to predict disease progression. Hence, there is an urgent clinical need for novel prognostic and therapeutic biomarkers.

High expression of NCS1 has been linked to poor outcomes in breast cancer patients as well as in patients suffering from liver cancer. Recent investigations suggest that high NCS1 levels accelerate metastatic spread of breast cancer by promoting crucial pro-metastatic capabilities. Moreover, previous in vitro studies provide strong evidence of increased cancer cell invasion, increased cancer cell survival and altered cancer cell adhesion due to high NCS1 levels. To test if these metastasis enhancing phenotypes also confer a functional effect in vivo, the effect of increased NCS1 on the metastatic capabilities of triple-negative breast cancer cells were investigated in a mouse xenograft model.

By utilizing a luciferase, photon-flux based, life imaging system, significantly accelerated lung metastasis formation by NCS1 overexpressing breast cancer cells, as compared to cells with a control level of NCS1, was demonstrated. Histopathological assessment of the developed lung metastases further delivered profound evidence that NCS1 overexpression facilitated early metastatic spread to the lungs and additionally increased cancer cell survival in mature metastases by preventing necrosis.

In an attempt to elucidate the metastasis promoting mechanisms, in vitro experiments were conducted. Herein, a migration favoring cellular phenotype of NCS1 overexpressing cells, as well as close association of NCS1 with actin in cellular protrusions, were successfully demonstrated. The observation of increased cell motility of NCS1 overexpressing cells in 2-D and 3-D motility assays confirmed a functional effect of this phenotype.

NCS1, as a calcium binding protein, plays a crucial role in calcium homeostasis. Calcium is by now recognized as an important second messenger in cancer progression and metastasis. Consequently, in this dissertation, the influence of NCS1 on the PI3K / AKT

pathway, the direct interaction of NCS1 with the InsP3R and the function of NCS1 in the LIMK1- pathway were suggested as possible routes through which NCS1 might promote cancer progression.

In sum, the investigations are supportive of the hypothesis that NCS1 increases metastatic capabilities of triple-negative breast cancer in vivo. Clinical evidence, as well as multiple in vitro and in vivo experiments suggest adverse outcomes for cancer patients with high NCS1 levels. Therefore, NCS1 might qualify as a novel prognostic biomarker for triple-negative breast cancer.

Previously reported interactions between NCS1 and chemotherapeutic drugs emphasize the relevance to further evaluate possible therapeutic targeting of NCS1 in cancer. This could lead to the discovery of urgently needed, novel pharmacologic therapy schemes in the treatment of triple-negative breast cancer.

1.7 References

Ando H, Kawaai K, Bonneau B, Mikoshiba K. Remodeling of Ca2+ signaling in cancer: regulation of inositol 1,4,5- trisphosphate receptors through oncogenes and tumor suppressors. Adv Biol Regul 2018; 68: 64-76

Apasu JE, Schuette D, LaRanger R, Steinle JA, Nguyen LD, Grosshans HK, Zhang M, Cai WL, Yan Q, Robert ME, Mak M, Ehrlich BE. Neuronal calcium sensor 1 (NCS1) promotes motility and metastatic spread of breast cancer cells in vitro and in vivo. FASEB J 2019; 33: 4802-4813

Balla A, Balla T. Phosphatidylinositol 4-kinases: old enzymes with emerging functions. Trends Cell Biol 2006; 16: 351-361

Becker S. A historic and scientific review of breast cancer: The next global healthcare challenge. Int J Gynaecol Obstet 2015; 131: S36-S39

Berridge MJ. Inositol trisphosphate and calcium signaling. Nature 1993; 361: 315-325

Berridge MJ. Neuronal calcium signaling. Neuron 1998; 21: 13-26

Blasiole B, Kabbani N, Boehmler W, Thisse B, Thisse C, Canfield V, Levenson R. Neuronal calcium sensor-1 gene ncs-1a is essential for semicircular canal formation in zebrafish inner ear. J Neurobiol 2005; 64: 285-297

Boeckel GR, Ehrlich BE. NCS-1 is a regulator of calcium signaling in health and disease. Biochim Biophys Acta Mol Cell Res 2018; 1865: 1660-1667

Boehmerle W, Splittgerber U, Lazarus MB, McKenzie KM, Johnston DG, Austin DJ, Ehrlich BE. Paclitaxel induces calcium oscillations via an inositol 1,4,5-trisphosphate receptor and neuronal calcium sensor 1-dependent mechanism. Proc Natl Acad Sci U S A 2006; 103: 18356-18361

Bong AHL, Robitaille M, Milevskiy MJG, Roberts-Thomson SJ, Monteith GR. NCS-1 expression is higher in basal breast cancers and regulates calcium influx and cytotoxic responses to doxorubicin. Mol Oncol 2020; 14: 87-104

Boye K, Maelandsmo GM. S100A4 and metastasis: a small actor playing many roles. Am J Pathol 2010; 176: 528-535

Cailleau R, Olivé M, Cruciger QV. Long-term human breast carcinoma cell lines of metastatic origin: preliminary characterization. In Vitro 1978; 14: 911-915

Chen YF, Chen YT, Chiu WT, Shen MR. Remodeling of calcium signaling in tumor progression. J Biomed Sci 2013; 20: 23

Choe CU, Ehrlich BE. The inositol 1,4,5-trisphosphate receptor (IP3R) and its regulators: sometimes good and sometimes bad teamwork. Sci STKE 2006; 2006: re15

Clapham DE. Calcium signaling. Cell 2007; 131: 1047-1058

Fantozzi A, Christofori G. Mouse models of breast cancer metastasis. Breast Cancer Res 2006; 8: 212

Fidler IJ. The pathogenesis of cancer metastasis: the 'seed and soil' hypothesis revisited. Nat Rev Cancer 2003; 3: 453-458

Fisher B, Anderson S, Bryant J, Margolese RG, Deutsch M, Fisher ER, Jeong JH, Wolmark N. Twenty-year follow-up of a randomized trial comparing total mastectomy, lumpectomy, and lumpectomy plus irradiation for the treatment of invasive breast cancer. N Engl J Med 2002; 347: 1233-1241

Friedl P, Gilmour D. Collective cell migration in morphogenesis, regeneration and cancer. Nat Rev Mol Cell Biol 2009; 10: 445-457

Gagliardi PA, Puliafito A, di Blasio L, Chianale F, Somale D, Seano G, Bussolino F, Primo L. Real-time monitoring of cell protrusion dynamics by impedance responses. Sci Rep 2015; 5: 10206

Gromada J, Bark C, Smidt K, Efanov AM, Janson J, Mandic SA, Webb DL, Zhang W, Meister B, Jeromin A, Berggren PO. Neuronal calcium sensor-1 potentiates glucose-dependent exocytosis in pancreatic beta cells through activation of phosphatidylinositol 4-kinase beta. Proc Natl Acad Sci U S A 2005; 102: 10303-10308

Grosshans HK, Fischer TT, Steinle JA, Brill AL, Ehrlich BE. Neuronal Calcium Sensor 1 is up-regulated in response to stress to promote cell survival and motility in cancer cells. Mol Oncol 2020; 14: 1134-1151

Gunter TE, Pfeiffer DR. Mechanisms by which mitochondria transport calcium. Am J Physiol 1990; 258: C755-C786

Gupta GP, Massagué J. Cancer Metastasis: Building a Framework. Cell 2006; 127: 679-695

Hajnoczky G, Davies E, Madesh M. Calcium signaling and apoptosis. Biochem Biophys Res Commun 2003; 304: 445-454

Han J, Yu J, Dai Y, Li J, Guo M, Song J, Zhou X. Overexpression of miR-361-5p in triple-negative breast cancer (TNBC) inhibits migration and invasion by targeting RQCD1 and inhibiting the EGFR/PI3K/Akt pathway. Bosn J Basic Med Sci 2019; 19: 52-59

Hanahan D, Weinberg RA. Hallmarks of cancer: the next generation. Cell 2011; 144: 646-674

Haynes LP, Fitzgerald DJ, Wareing B, O'Callaghan DW, Morgan A, Burgoyne RD. Analysis of the interacting partners of the neuronal calcium-binding proteins L-CaBP1, hippocalcin, NCS-1 and neurocalcin delta. Proteomics 2006; 6: 1822-1832

Hseu YC, Lin YC, Rajendran P, Thigarajan V, Mathew DC, Lin KY, Way TD, Liao JW, Yang HL. Antrodia salmonea suppresses invasion and metastasis in triple-negative breast cancer cells by reversing EMT through the NF-κB and Wnt/β-catenin signaling pathway. Food Chem Toxicol 2019; 124: 219-230

Hudis CA, Gianni L. Triple-negative breast cancer: an unmet medical need. Oncologist 2011; 16: S1-S11

Koizumi S, Rosa P, Willars GB, Challiss RA, Taverna E, Francolini M, Bootman MD, Lipp P, Inoue K, Roder J, Jeromin A. Mechanisms underlying the neuronal calcium sensor-1-evoked enhancement of exocytosis in PC12 cells. J Biol Chem 2002; 277: 30315-30324

Lambert AW, Pattabiraman DR, Weinberg RA. Emerging biological principles of metastasis. Cell 2017; 168: 670-691

Lee YTM. Patterns of metastasis and natural courses of breast carcinoma. Cancer Metastasis Rev 1985; 4: 153-172

Li R, Doherty J, Antonipillai J, Chen S, Devlin M, Visser K, Baell J, Street I, Anderson RL, Bernard O. LIM kinase inhibition reduces breast cancer growth and invasiveness but systemic inhibition does not reduce metastasis in mice. Clin Exp Metastasis 2013; 30: 483-495

Lim E, Modi KD, Kim J. In vivo bioluminescent imaging of mammary tumors using IVIS spectrum. J Vis Exp 2009; 26: 1210

Livak KJ, Schmittgen TD. Analysis of relative gene expression data using real-time quantitative PCR and the 2(-Delta Delta C(T)) Method. Methods 2001; 25: 402-408

Mehlen P, Puisieux A. Metastasis: a question of life or death. Nat Rev Cancer 2006; 6: 449-458

Mo M, Erdelyi I, Szigeti-Buck K, Benbow JH, Ehrlich BE. Prevention of paclitaxel-induced peripheral neuropathy by lithium pretreatment. FASEB J 2012; 26: 4696-4709

Moore LM, England A, Ehrlich BE, Rimm DL. Calcium sensor, NCS-1, promotes tumor aggressiveness and predicts patient survival. Mol Cancer Res 2017; 15: 942-952

Nakamura TY, Jeromin A, Smith G, Kurushima H, Koga H, Nakabeppu Y, Wakabayashi S, Nabekura J. Novel role of neuronal Ca2+ sensor-1 as a survival factor up-regulated in injured neurons. J Cell Biol 2006; 172: 1081-1091

Nguyen LD, Petri ET, Huynh LK, Ehrlich BE. Characterization of NCS1-InsP3R1 interaction and its functional significance. J Biol Chem 2019; 294: 18923-18933

Nguyen T, Chin WC, Verdugo P. Role of Ca2+/K+ ion exchange in intracellular storage and release of Ca2+. Nature 1998; 395: 908-912

Pantel K, Brakenhoff RH. Dissecting the metastatic cascade. Nat Rev Cancer 2004; 4: 448-456

Pelleitier M, Montplaisir S. The nude mouse: a model of deficient T-cell function. Methods Achiev Exp Pathol 1975; 7: 149-166

Pettit EJ, Fay FS. Cytosolic free calcium and the cytoskeleton in the control of leukocyte chemotaxis. Physiol Rev 1998; 78: 949-967

Ponomarev V, Doubrovin M, Serganova I, Vider J, Shavrin A, Beresten T, Ivanova A, Ageyeva L, Tourkova V, Balatoni J, Bornmann W, Blasberg R, Gelovani Tjuvajev J. A novel triple-modality reporter gene for whole-body fluorescent, bioluminescent, and nuclear noninvasive imaging. Eur J Nucl Med Mol Imaging 2004; 31: 740-751

Prevarskaya N, Skryma R, Shuba Y. Calcium in tumor metastasis: new roles for known actors. Nat Rev Cancer 2011; 11: 609-618

Rajebhosale M, Greenwood S, Vidugiriene J, Jeromin A, Hilfiker S. Phosphatidylinositol 4-OH kinase is a downstream target of neuronal calcium sensor-1 in enhancing exocytosis in neuroendocrine cells. J Biol Chem 2003 21; 278: 6075-6084

Riching KM, Cox BL, Salick MR, Pehlke C, Riching AS, Ponik SM, Bass BR, Crone WC, Jiang Y, Weaver AM, Eliceiri KW, Keely PJ. 3D collagen alignment limits protrusions to enhance breast cancer cell persistence. Biophys J 2014; 107: 2546-2558

Schaad NC, De Castro E, Nef S, Hegi S, Hinrichsen R, Martone ME, Ellisman MH, Sikkink R, Rusnak F, Sygush J, Nef P. Direct modulation of calmodulin targets by the neuronal calcium sensor NCS-1. Proc Natl Acad Sci U S A 1996; 93: 9253-9258

Schlecker C, Boehmerle W, Jeromin A, DeGray B, Varshney A, Sharma Y, Szigeti-Buck K, Ehrlich BE. Neuronal calcium sensor-1 enhancement of InsP3 receptor activity is inhibited by therapeutic levels of lithium. J Clin Invest 2006; 116: 1668-1674

Schuette D, Moore LM, Robert ME, Taddei TH, Ehrlich BE. Hepatocellular carcinoma outcome is predicted by expression of neuronal calcium sensor 1. Cancer Epidemiol Biomarkers Prev 2018; 27: 1091-1100

Scott RW, Hooper S, Crighton D, Li A, König I, Munro J, Trivier E, Wickman G, Morin P, Croft DR, Dawson J, Machesky L, Anderson KI, Sahai EA, Olson MF. LIM kinases are required for invasive path generation by tumor and tumor- associated stromal cells. J Cell Biol 2010; 191: 169-185

Scott RW, Olson MF. LIM kinases: function, regulation and association with human disease. J Mol Med (Berl) 2007; 85: 555-568

Stewart TA, Yapa KT, Monteith GR. Altered calcium signaling in cancer cells. Biochim Biophys Acta 2015; 1848: 2502-2511

Stuelten CH, Parent CA, Montell DJ. Cell motility in cancer invasion and metastasis: insights from simple model organisms. Nat Rev Cancer 2018; 18: 296-312

Tarabykina S, Griffiths TR, Tulchinsky E, Mellon JK, Bronstein IB, Kriajevska M. Metastasis-associated protein S100A4: spotlight on its role in cell migration. Curr Cancer Drug Targets 2007; 7: 217-228

Vivanco I, Sawyers CL. The phosphatidylinositol 3- kinase AKT pathway in human cancer. Nat Rev Cancer 2002; 2: 489-501

Waks AG, Winer EP. Breast cancer treatment: a review. JAMA 2019; 321: 288-300

Weiss JL, Archer DA, Burgoyne RD. Neuronal Ca2+ sensor-1/frequenin functions in an autocrine pathway regulating Ca2+ channels in bovine adrenal chromaffin cells. J Biol Chem 2000; 275: 40082-40087

Weiss JL, Hui H, Burgoyne RD. Neuronal calcium sensor-1 regulation of calcium channels, secretion, and neuronal outgrowth. Cell Mol Neurobiol 2010; 30: 1283-1292

Wu PH, Giri A, Sun SX, Wirtz D. Three-dimensional cell migration does not follow a random walk. Proc Natl Acad Sci U S A 2014; 111: 3949-3954

Xiao M, Li T, Ji Y, Jiang F, Ni W, Zhu J, Bao B, Lu C, Ni R. S100A11 promotes human pancreatic cancer PANC-1 cell proliferation and is involved in the PI3K/AKT signaling pathway. Oncol Lett 2018; 15: 175-182

Yamaguchi H, Condeelis J. Regulation of the actin cytoskeleton in cancer cell migration and invasion. Biochim Biophys Acta 2007; 1773: 642-652

Zhang Y, Zhao Z, Li S, Dong L, Li Y, Mao Y, Liang Y, Tao Y, Ma J. Inhibition of miR-214 attenuates the migration and invasion of triple-negative breast cancer cells. Mol Med Rep 2019; 19: 4035-4042

Zheng JQ, Poo MM. Calcium signaling in neuronal motility. Annu Rev Cell Dev Biol 2007; 23: 375-404

2. Publication

THE FASEB JOURNAL • RESEARCH • www.fasebj.org

Neuronal calcium sensor 1 (NCS1) promotes motility and metastatic spread of breast cancer cells *in vitro* and *in vivo*

Jonathan E. Apasu,*[,1] Daniel Schuette,* Ryan LaRanger,[†] Julia A. Steinle,*[,2] Lien D. Nguyen,* Henrike K. Grosshans,* Meiling Zhang,[‡] Wesley L. Cai,[‡] Qin Yan,[‡] Marie E. Robert,[‡] Michael Mak,[†] and Barbara E. Ehrlich*[,3]

*Department of Pharmacology, [†]Department of Biomedical Engineering, and [‡]Department of Pathology, Yale University, New Haven, Connecticut, USA

ABSTRACT: Increased levels of the calcium-binding protein neuronal calcium sensor 1 (NCS1) predict an unfavorable patient outcome in several aggressive cancers, including breast and liver tumors. Previous studies suggest that NCS1 overexpression facilitates metastatic spread of these cancers. To investigate this hypothesis, we explored the effects of NCS1 overexpression on cell proliferation, survival, and migration patterns *in vitro* in 2- and 3-dimensional (2/3-D). Furthermore, we translated our results into an *in vivo* mouse xenograft model. Cell-based proliferation assays were used to demonstrate the effects of overexpression of NCS1 on growth rates. *In vitro* colony formation and wound healing experiments were performed and 3-D migration dynamics were studied using collagen gels. Nude mice were injected with breast cancer cells to monitor NCS1-dependent metastasis formation over time. We observed that increased NCS1 levels do not change cellular growth rates, but do significantly increase 2- and 3-D migration dynamics *in vitro*. Likewise, NCS1-overexpressing cells have an increased capacity to form distant metastases and demonstrate better survival and less necrosis *in vivo*. We found that NCS1 preferentially localizes to the leading edge of cells and overexpression increases the motility of cancer cells. Furthermore, this phenotype is correlated with an increased number of metastases in a xenograft model. These results lay the foundation for exploring the relevance of an NCS1-mediated pathway as a metastatic biomarker and as a target for pharmacologic interventions.—Apasu, J. E., Schuette, D., LaRanger, R., Steinle, J. A., Nguyen, L. D., Grosshans, H. K., Zhang, M., Cai, W. L., Yan, Q., Robert, M. E., Mak, M., Ehrlich, B. E. Neuronal calcium sensor 1 (NCS1) promotes motility and metastatic spread of breast cancer cells *in vitro* and *in vivo*. FASEB J. 33, 4802–4813 (2019). www.fasebj.org

KEY WORDS: cell migration · xenograft model · calcium binding protein · metastasis · Ca^{2+} signaling

A hallmark of aggressive tumors is their ability to invade tissues and metastasize to distant organs (1). It is well known that the majority of tumor-related deaths are attributable to dissemination of cancer cells throughout the body (2, 3). Nevertheless, many of the mechanisms that favor the spread of tumor cells to distant sites in the body remain to be elucidated (1, 4).

Calcium (Ca^{2+}) is a crucial second messenger molecule. It enters the cytoplasm *via* voltage- or ligand-gated channels (5, 6) from 2 major sources, the extracellular space and intracellular Ca^{2+} storage compartments such as the endoplasmic reticulum (7) and the mitochondria (8). Release of Ca^{2+} from intracellular compartments often follows oscillatory patterns, which can lead to reprogramming of the transcriptional machinery of mammalian cells (9–11). Alterations in cytoplasmic Ca^{2+} regulate critical cellular processes such as proliferation, cell growth, cell cycle progression (12), neurogenesis (6, 13, 14), and apoptotic cell death (12, 15).

The coordinated movement of cells largely depends on tightly regulated spatiotemporal Ca^{2+} signals (16–20). Given these properties of the physiologic function of Ca^{2+}, dysregulated Ca^{2+} pathways were recently recognized to be possible drivers of aggressive, highly metastatic cancers (21–24). A variety of proteins that are involved in regulating and amplifying Ca^{2+} signals in mammalian cells have been implicated in cancer progression, including

ABBREVIATIONS: 2/3-D, 2-dimensional; GFP, green fluorescent protein; H&E, hematoxylin and eosin; HEK-293, human embryonic kidney 293; IHC, immunohistochemistry; InsP3R, inositol 1,4,5-*tris*phosphate receptor; MSD, mean squared displacement; NCS1, neuronal calcium sensor 1; NCS1-OE, NCS1-overexpressing; PI4K, phosphatidylinositol 4-OH kinase

[1] Current affiliation: University of Bonn, Bonn, Germany.
[2] Current affiliation: University of Muenster, Muenster, Germany.
[3] Correspondence: Department of Pharmacology, Yale University, 333 Cedar St., Room B-147, P.O. Box 208026, New Haven, CT 06520-8066, USA. E-mail: barbara.ehrlich@yale.edu

doi: 10.1096/fj.201802004R
This article includes supplemental data. Please visit *http://www.fasebj.org* to obtain this information.

0892-6638/19/0033-4802 © FASEB

S100 Ca^{2+}-binding proteins (25) and visinin-like protein 1 (VILIP1) (26). The fact that cell motility is regulated by Ca^{2+} as a second messenger suggests that molecules which bind Ca^{2+} and mediate its downstream effects could be potential cancer biomarkers as well as therapeutic targets.

One example of a Ca^{2+} regulated kinase involved in cell movement is LIM domain kinase 1 (LIMK1) (16). LIMK1 regulates the organization of the actin cytoskeleton *via* phosphorylation of its downstream effector cofilin (27). Cancer cells rely on increased levels of LIMK1 to be able to invade the tissue that surrounds the tumor (28) and inhibition of LIMK1 reduces their invasiveness (29, 30).

Neuronal calcium sensor 1 (NCS1) is a ubiquitously expressed Ca^{2+} binding protein (31, 32) with the highest levels of expression being found in the CNS (33). It is closely related to other members of the NCS family of proteins (34) such as hippocalcin or recoverin. On the structural level, NCS proteins are composed of 4 EF-hand domains that are canonical Ca^{2+} binding sites and a myristoylation site at the N terminus (31). NCS1 interacts with a wide range of proteins, including the inositol 1,4,5-*tris*phosphate receptor (InsP3R), dopamine receptor type 2 (D2R), and phosphatidylinositol 4-OH kinase (PI4K) (35, 36). Through its protein–protein interactions, NCS1 regulates vital cellular processes such as neurotransmitter release (32), neurite outgrowth and neuronal survival (37, 38), spatial memory formation (31), and the InsP3R signaling pathway (39, 40).

We have previously described NCS1 as a prognostic biomarker in cohorts of breast (41) and liver (42) cancer patients and demonstrated that the overexpression of NCS1 leads to a marked increase in invasion and motility *in vitro* (41) using 2-dimensional (2-D) assays. Furthermore, NCS1 expression levels are highly correlated with other components of Ca^{2+} signaling as well as LIMK1 expression (42). In this study, we investigated the hypothesis that increased expression of NCS1 facilitates the formation of distant metastases by enhancing cellular motility. *In vitro* cell culture models of NCS1 overexpression were used to demonstrate that NCS1 levels do not modulate proliferation rates but do modulate cell motility in 2- and 3-D environments. We validated these results in a mouse model, showing that NCS1 facilitates early metastatic spread of tumor cells and increases the survival of cancer cells in more mature tumors.

MATERIALS AND METHODS

Cell culturing

MDA-MB-231 cells were obtained from the American Type Culture Collection (ATCC; Manassas, VA, USA). ATCC validates all cell lines by Short Tandem Repeat Analysis. The MDA-MB-231 cells were transduced with a NCS1 overexpression vector and a control vector as previously described (41). The MDA-MB-231 cell lines were maintained at 37°C, 5% CO_2 in DMEM medium supplemented with 10% fetal bovine serum, 1% L-glutamine and 1% penicillin/streptomycin.

Cell proliferation assays

For the CellTiter-Glo assay, 1000 cells/well were plated into sterile 96-well plates and grown over a period of 5 d. The relative number of viable cells was determined every day for 10 wells of such a plate using CellTiter-Glo reagent (Promega, Madison, WI, USA) and a microplate reader (Tecan Infinite M1000 Pro; Tecan Trading, Männedorf, Switzerland) according to the manufacturers' instructions. Every well was used just once and the marginal wells were never used. Three independent experiments were performed using NCS1-overexpressing (OE) MDA-MB-231 cells and control cells, and all measurements were normalized to the average luminescence on d 1.

For the AlamarBlue assay, 8 replicates of 1250, 2500, 5000, and 10,000 cells/well were plated into sterile 96-well plates. After a 24-h incubation period, medium was removed and 100 μl fresh medium with an additional 10 μl AlamarBlue reagent (Thermo Fisher Scientific, Waltham, MA, USA) was added to each well. After another 2 h of incubation, a fluorescence signal was measured using the aforementioned microplate reader.

Scratch assay and colony formation assay

Scratch assays were performed as previously described (41). Cells were serum starved 12 h prior to the experiment to inhibit cell proliferation. For quantification, ImageJ (National Institutes of Health, Bethesda, MD, USA) was used and the distance traveled was calculated after 24 h. The mean distance traveled was plotted for $n = 3$ independent experiments.

For colony formation assays, cells were cultured per standard protocol in T75 flasks. Once cell confluence approached 80–90%, the cells were detached by the addition of 2 ml TrypLE (Thermo Fisher Scientific, Rockford, IL, USA), followed by dilution in 5 ml of fresh medium. Cell concentration was determined using a hematocytometer. Subsequently, a total number of 100, 200 or 500 cells was added to each well of a 12-well plate. Cells were then left undisturbed in the incubator for 14 d. After 14 d, colonies were fixed and stained with 2.5% crystal violet solution and were subsequently washed to remove excess dye and scanned with a conventional scanner. The total area covered was determined with ImageJ (43). Data were obtained from 3 independent experiments with 4 replicates in each experiment. Data were represented as total area covered in each individual well.

Quantitative RT-PCR

RNA was isolated using the RNeasy Mini Kit (Qiagen, Hilden, Germany) according to the manufacturer's instructions. Using a High-Capacity cDNA Reverse Transcription Kit (4368814; Thermo Fisher Scientific) according to the manufacturer's protocol, 0.5–1 μg of RNA was then transcribed to cDNA. Quantitative real-time PCR was performed using Power SYBR Green Master Mix reagent and a 7300 Real-Time PCR System (Thermo Fisher Scientific). The $\Delta\Delta C_t$ method (44) was used to calculate expression fold changes with ACTB (β-actin) and ribosomal protein S18 as control genes. The following primers were used at a concentration of 5 μM: NCS1 (forward, 5′-GATGCTGGACATTGTGGATG-3′; reverse, 5′-CTTGGAACCCTCCTGGAACT-3′), ACTB (forward, 5′-GTCTTCCCCTCCATCGTGG-3′; reverse, 5′-GATGCCTCTCTTGCTCTGGG-3′), and S18 (forward, 5′-TTCGAACGTCTGCCCTATCAA-3′; reverse, 5′-ATGGTAGGCACGGCGACTA-3′).

Assessment of NCS1 protein levels

MDA-MB-231 cells were lysed in ice-cold M-PER Mammalian Protein Extraction Reagent buffer (Thermo Fisher Scientific) supplemented with a protease inhibitor. Protein concentrations were determined using the Bio-Rad protein assay reagent (San Diego, CA, USA). SDS-PAGE was performed with 30 μg of protein. Briefly, the protein was transferred to a nitrocellulose membrane (GE Healthcare, Chicago, IL, USA), the resulting blots were blocked for 1 h in 5% nonfat dry milk in Tris-buffered saline with 0.1% Tween 20 (TBST), and were then incubated with a primary NCS1-specific antibody (sc-13037, diluted 1:5000; Santa Cruz Biotechnology, Dallas, TX, USA) or β-actin–specific antibody (sc-47778, diluted 1:1000; Santa Cruz Biotechnology) over night at 4°C. All dilutions are vol/vol. Blots were then incubated with horseradish peroxidase and labeled goat anti-rabbit IgG (diluted 1:10,000; Santa Cruz Biotechnology) at room temperature for 1 h. Ultimately, protein bands were visualized using electrochemiluminescence detection reagents (Thermo Fisher Scientific).

Immunofluorescence microscopy

Control and NCS1-OE cells were seeded on sterile 22 × 22-mm glass coverslips at a density of 50,000 cells/coverslip. Medium was removed 24 h after seeding, and each coverslip was briefly washed twice with 2 ml of 1× PBS (pH 7.4; AmericanBio, Natick, MA, USA) each time. Fixation was performed for 15 min at room temperature with a 4% paraformaldehyde solution (pH 7.4). Following 3 washes with 2 ml PBS, cells were permeabilized and blocked in PBS solution containing 1% bovine serum albumin (0.1% Triton-X 100; AmericanBio) for 1 h at room temperature. Following blocking, cells were incubated with a rabbit anti-NCS1 pAb diluted in blocking solution (sc-13037, diluted 1:100; Santa Cruz Biotechnology) overnight at 4°C. After extensive washing with PBS, cells were incubated with an AlexaFluor-488 goat anti-rabbit secondary antibody (diluted 1:1000; Thermo Fisher Scientific) and a rhodamine-conjugated phalloidin (diluted 1:1000 dilution; Thermo Fisher Scientific) for 2 h at room temperature in the dark. Cells were then washed extensively with PBS before being mounted on glass slides with antifade medium ProLong Gold with DAPI (Thermo Fisher Scientific). Slides were cured overnight before images were captured with a confocal microscope using the ×100 lens (LSM 710 Duo; Carl Zeiss, Oberkochen, Germany). A laser power of 0.5% was used to detect NCS1 in overexpressing cells and 10% to detect NCS1 in control cells. All other settings were kept the same among all coverslips.

Transduction of cells with a reporter for bioluminescent imaging

Previously (41) generated NCS1-OE and control MDA-MB-231 cells were retro-virally infected with a triple-fusion protein reporter. The reporter encodes for herpes simplex virus thymidine kinase 1, green fluorescent protein (GFP) and firefly luciferase (45). Human embryonic kidney 293 (HEK-293) cells were used to produce viruses. They were transduced using the Clontech Calcium Phosphate Transfection Kit (Clontech Laboratories, Mountain View, CA, USA) and a polybrene-facilitated infection of MDA-MB-231 cells. Briefly, HEK-293 cells were plated on a 10 cm dish 1 d before the transfection for producing retrovirus and grown to 60% confluence. The next day, 20 μg of retroviral vector DNA and packaging plasmids [envelope, vesicular stomatitis virus (VSVG) 6 μg; 10μg pMDLg/pRRE 3rd generation lentiviral packaging plasmid containing Gag and Pol, 5μg pRSV-Rev 3rd generation lentiviral packaging plasmid containing Rev (or HIV1gp6)] were mixed with 4-(2-hydroxyethyl)-1-piperazineethanesulfonic acid–buffered saline to obtain a 1-time solution and were then incubated for 15 min. Then, the plasmid-containing solution was added drop-wise to the HEK-293 cells and fresh medium was applied after 6 h. The HEK-293 cells were examined for GFP positivity 2 d after transfection by using a microscope to measure green fluorescence. The retrovirus-containing supernatant was collected on d 2 and 3 after transfection and was centrifuged and filtered using a 0.45-μm filter.

MDA-MB-231 cells were incubated with the virus-containing solution and 4 μg/ml polybrene for 6 h. The medium was changed after the 6 h incubation and later on d 4. On d 6, the MDA-MB-231 cells were checked for GFP expression. The MDA-MB-231 cells were harvested 48 h posttransduction in ice-cold PBS and were passed through a 70-μM filter. After 2 washing cycles, cells were prepared in PBS at a concentration of 5–10 million/ml. Cells were sorted for GFP positivity using a FACSAria-B high-speed cell sorter (BD Biosciences, San Jose, CA, USA). GFP positive cells were collected and transferred to a sterile plastic flask for further culturing.

Assessment of bioluminescence

The Promega Luciferase Assay System was used to quantify bioluminescence. Cells were prepared in a 96-well plate according to the manufacturer's instructions. Luciferin was added to the wells 20 s before measuring luminescence using a Tecan Infinite M1000 Pro microplate reader.

Cell migration assay

Embedding MDA-MB-231 cancer cells in a 3-D collagen I matrix

Engineered MDA-MB-231 cells were suspended at a concentration of 10 million cells/ml in tissue culture media. A collagen gel was made by adding a calculated amount of 0.5 N NaOH to neutralize a mixture of double-distilled H_2O and acetic acid–solubilized type I rat tail collagen (Corning, Corning, NY, USA) on ice for a final collagen concentration of 4 mg/ml. Suspended cells were then added to the gel at a 1:10 dilution for a final cell concentration of 1×10^6 cells/ml. The gels were then transferred to a 24-well glass-bottomed cell culture plate (MatTek, Ashland, MA, USA) kept on an ice pack. Once all gels were transferred to the 24-well plate, the plate was transferred to an incubator at 37°C with 5% CO_2. The sample was flipped several times during gelation to prevent cell sediment from forming on the bottom of the plate. After 1 h, tissue culture media was added to the gels, which were subsequently maintained at 37°C with 5% CO_2.

Analysis of cell shape, velocity, and mean squared displacement

A Leica SP8 confocal microscope (Wetzlar, Germany) using a ×20 objective was used to image the cells. A temperature of 37°C and a 5% CO_2 atmosphere were maintained using a humidified OKO labs live cell imaging incubator. For each well, 250 μm z stacks were created using 10 slices ≥50 μm from the bottom of the well. Images were taken every 5 min for 8 h to create the final hyperstacks. The perimeter, circularity, and aspect ratio of the cells were measured by tracing the edges of z projections of 20 cells using ImageJ. Cell migration was tracked by first taking a z projection of the hyperstack to create a 2-D representation of 3-D migration of the cells. Cell migration was then manually tracked using the point selection tool in ImageJ across 8 h of hyperstack data. The resulting output was analyzed using custom scripts in MatLab (MathWorks, Natick, MA, USA). The average speed of

each condition was determined by measuring the average speed of each cell at each time step, and then averaging this average cell speed for 40 cells across all conditions. The mean squared displacement (MSD) was calculated as

$$\mathrm{MSD}(\Delta t) = < [x(t+\Delta t) - x(t)]^2 + [y(t+\Delta t) - y(t)]^2 >$$

where Δt is time interval, $x(t)$ and $y(t)$ are spatial coordinates at time t, and $< \ldots >$ indicates the average over all available starting times. An average of the MSDs at the longest interval (8 h) was calculated for 40 cells per condition. Static trajectories and graphs of MSDs were also created using custom scripts in MatLab.

Animal studies: tail vein injection

All mouse work was done in accordance with the Yale University Institutional Animal Care and Use Committee. Female athymic nude mice (7–9 wk old) were obtained from Envigo (Somerset, NJ, USA) for the xenografting study. For each mouse, 4×10^5 MDA-MB-231 cells were harvested, washed in PBS, resuspended in 0.1 ml sterile saline, and injected into the lateral tail vein. The mice were imaged directly after the tail vein injection and unsuccessfully xenografted mice were excluded from the study.

Mouse imaging studies, data analysis, and lung harvest

After anesthetizing mice by intraperitoneal injection of 0.2 ml 10% ketamine/1% xylazine in sterile saline, they were retro-orbitally injected with 0.1 ml luciferin. The mice were imaged within 2–5 min of the retro-orbital injection using a Perkin-Elmer Ivis system coupled with Live Image acquisition and analysis software. The photon flux from the xenografted cells in the lungs of each mouse was evaluated by selecting a rectangular region of interest over the lung. All obtained values were normalized to the photon flux obtained immediately after xenografting, resulting in an initial bioluminescence signal of 1 for every mouse.

Lungs for histopathologic evaluation were harvested on d 3 and 7 and at the end of the study. The lungs were harvested after the aforementioned *in vivo* imaging of xenografted mice and after perfusion with 10 ml ice-cold Dulbecco's PBS. The harvested lungs were washed in ice-cold Dulbecco's PBS and imaged with Ivis to obtain an *ex-vivo* lung bioluminescence signal.

Histopathologic assessment of lung specimens

Harvested lung tissue was placed in 10% formalin for fixation. After fixation, the lungs were paraffin embedded and hematoxylin and eosin (H&E)–stained slides were generated by Yale Mouse Pathology. Anti-NCS1 immunohistochemical staining using a previously described antibody (41) was performed by Yale Research Histology to confirm the presence of human NCS1-positive MDA-MB-231 cells in the xenografted lungs. All slides underwent blind evaluation by an experienced pathologist.

Statistical analysis

Unless noted otherwise, all analyses were done using the Python programming language (v.3.6; *https://www.python.org/*). An independent 2-sample Student's t test was used to compare the mean values of 2 independent datasets; values of $P < 0.05$ were considered significant. Whenever possible, error bars were plotted indicating either 95% confidence intervals or the means ± SEM.

RESULTS

Overexpression of NCS1 changes the cellular phenotype without affecting proliferation rates

To explore the *in vitro* function of NCS1 in malignant tumors, we stably overexpressed NCS1 in MDA-MB-231 breast cancer cells (referred to as NCS1-OE) using a previously described protocol (41). Immunoblotting was performed to confirm successful overexpression of the target gene (**Fig. 1*A***). Real-time quantitative PCR measurements confirmed that NCS1 mRNA expression levels were, on average, 4-fold higher in NCS1-OE cells than in the controls. This result was consistent when normalized to 2 different housekeeping genes ($P < 0.01$, Supplemental Fig. S1).

To determine whether NCS1 overexpression enhances the aggressiveness of tumor cells by increasing their proliferation rates, cell growth of NCS1-OE and control cells was measured over a period of 5 d (Fig. 1*B*) using an ATP-based growth assay. As expected from previously reported results (41), no differences in proliferation rates were observed. To validate this result, we performed an AlamarBlue assay (Supplemental Fig. S2). Again, proliferation rates of NCS1-OE and control cells were similar. During the course of these experiments it became clear that the overexpression of NCS1 led to a marked change in cellular morphology in a 3-D environment (Fig. 1*C*). Specifically, NCS1-OE cells were significantly less rounded with a higher aspect ratio than the control (**$P < 0.01$, ***$P < 0.001$, Fig. 1*D*). Furthermore, NCS1-OE cells had a significantly higher cell perimeter (Supplemental Fig. S3). Large cellular protrusions were seen exclusively in the NCS1-OE context (Supplemental Fig. S4), suggesting that this newly acquired phenotype predicts the functional consequences of cellular motility, metastatic behavior, and survival (46, 47).

Immunofluorescence microscopy shows that NCS1 preferentially localizes to cell protrusions in control and NCS1-OE cells

To further investigate the localization of NCS1 in control and NCS1-OE MDA-MB231 cells, immunofluorescence imaging was performed (**Fig. 2*A, B***). As a result, NCS1 was found to be localized at cellular protrusions, including the lamellopodia. NCS1 also colocalizes extensively with actin at the leading edge, but not with cytoplasmic actin puncta or stress fibers.

NCS1 overexpression increases colony formation and cell motility in 2- and 3-D *in vitro* assays

To further investigate the hypothesis that NCS1 favors tumor growth and metastatic spread through increasing survival and motility instead of proliferation, a colony formation assay was performed. Different numbers of cells were plated in a cell culture dish and grown for 14 d. After

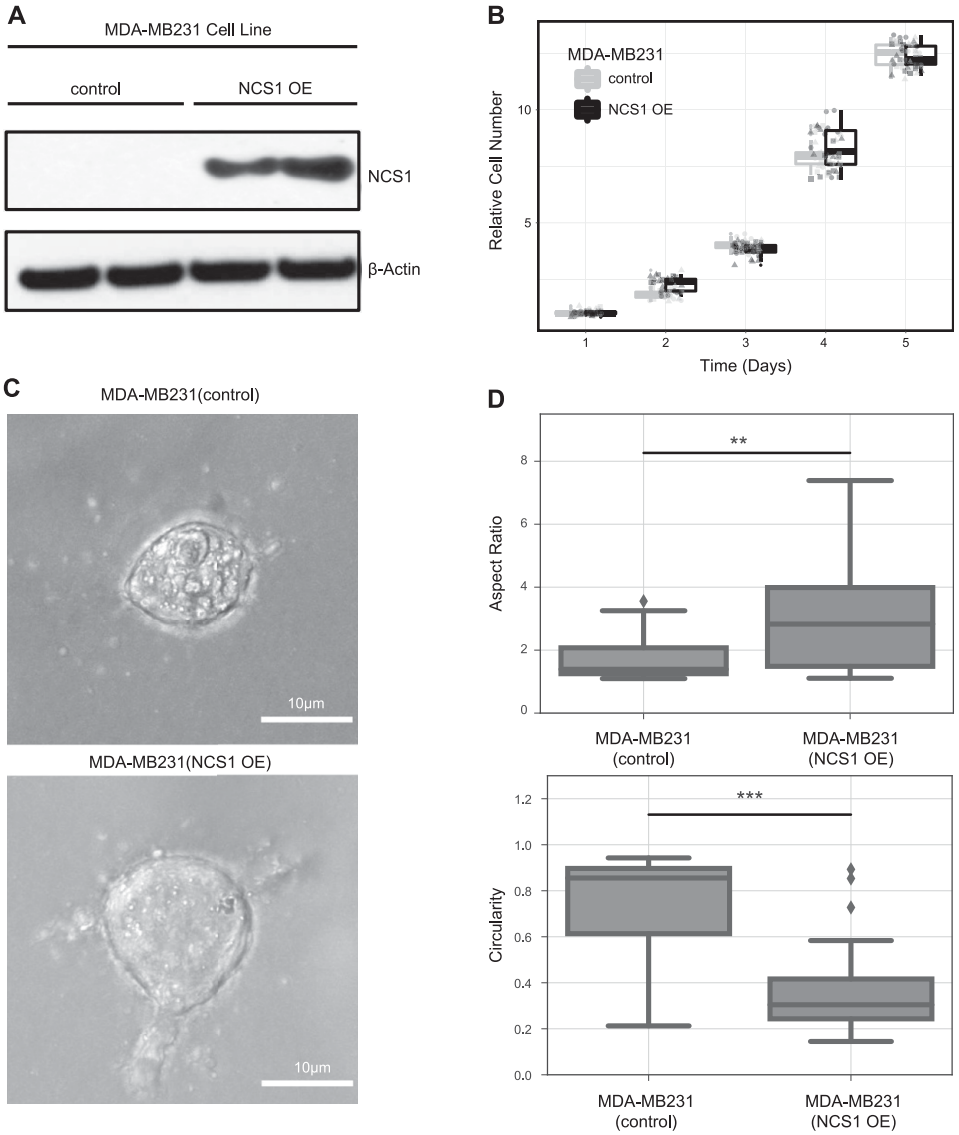

Figure 1. NCS1 overexpression changes cellular morphology of MDA-MB231 cells without affecting proliferation rates. *A*) Immunoblot showing control and NCS1-OE MDA-MB231 cells. Actin is used as a loading control. Longer exposure shows NCS1 expression in control cells, as previously demonstrated (41). *B*) Box plots demonstrating proliferation rates of MDA-MB231 control and NCS1-OE cells continuously over 5 d. Circles, triangles, and squares represent different biologic replicates. An ATP dye was used to measure the absolute cell number and all values were normalized to the mean on d 0 before plotting. *C*) Brightfield microscopy images of single MDA-MB231 control and NCS1-OE cells showing the different morphologies of these genotypes. Cells were grown in 3-D collagen gels identical to the gels used for subsequent experiments (*e.g.*, Fig. 3*C–E*). *D*) Box plots showing the aspect ratio and circularity of MDA-MB231 control and NCS1-OE cells ($n = 20$). $^{**}P < 0.01$, $^{***}P < 0.001$.

fixing and staining the resulting colonies, the total area covered by cells was calculated. Compared with the control, the NCS1-OE cells showed a significantly increased ability to form colonies ($P < 0.01$; **Fig. 3*A***). These differences were consistently found with different starting cell numbers (Fig. 3*A*). Thus, high NCS1 expression increases the capacity of cancer cells to form colonies *in vitro*, which mimics a metastatic setting.

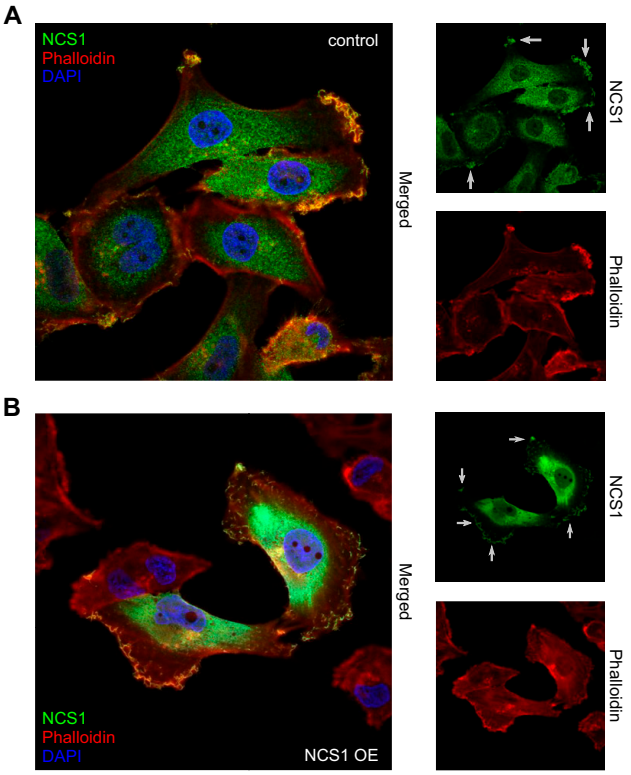

Figure 2. NCS1 localizes to the leading edge of MDA-MB231 control and NCS1-OE cells. *A*) Immunofluorescence microscopy image of control MDA-MB231 cells. The large panel shows a merged image of DAPI (blue), phalloidin (to stain for actin; red), and anti-NCS1 (green) stainings. The smaller panels show the same anti-NCS1 and Phalloidin stainings but separately. Small gray arrows point at localized NCS1. *B*) Immunofluorescence microscopy image of NCS1-OE MDA-MB231 cells. The large panel shows a merged image of DAPI (blue), Phalloidin (red), and anti-NCS1 (green) stainings. The smaller panels show the same anti-NCS1 and Phalloidin stainings but separately. Small gray arrows point at localized NCS1. Note that the laser power used to image the control cells in *A* was the original magnification and is ×20 larger than the NCS1-OE cells in *B*.

To monitor *in vitro* 2-D motility, assay cells were placed in a cell culture dish and a standardized wound was applied to the cell monolayer. Then, wound closure was quantified using the relative distance that control and NCS1-OE cells had traveled after 24 h. NCS1-OE cells closed the scratched area in the monolayer significantly ($P < 0.01$) more than the control cells, indicating an enhanced 2-D migration of NCS1-OE cells (Fig. 3*B*).

Next, a 3-D migration assay was performed to validate these findings. NCS1-OE and control MDA-MB231 cells were placed in a collagen matrix and time-lapse microscopy was performed to capture the movement of many cells simultaneously over time. The overall trajectory of 20 cells per condition is shown in Fig. 3*C*, where each colored trace is a single cell that was tracked over time, demonstrating that there was considerably more movement in the NCS1-OE condition. This movement did not have a directional bias. NCS1-OE cells showed increased MSD after 8 h, indicating that the NCS1-OE cells experienced significantly more net displacement ($P < 0.005$; Fig. 3*D*). Also, the average cell velocity in the NCS1-OE cells was significantly higher than in the control cells ($P < 0.001$; Fig. 3*E*). These results show that the NCS1-OE cells are better able to migrate through a 3-D collagen gel, which indicates that these cells would be more prone to metastatic migration *in vivo*.

NCS1-OE cells exhibit an increased capacity to metastasize *in vivo*

Given these changes in cellular phenotype, colony formation, and migratory capacity that are induced by overexpression of NCS1, we next studied NCS1 in an *in vivo* setting. Female nude mice were injected with MDA-MB231 cells that were engineered to express a firefly luciferase reporter and either NCS1 ($NCS1^+$) or an empty vector (control). Photon flux was utilized as a metric of relative tumor amount in the mouse lungs. The total flux was calculated from lung imaging studies on d 0, 1, 3, 7, 14, 21, and 28 (**Fig. 4*A***) after tail vein injection with the respective tumor cells. The majority of cells were observed in the lungs. No luminescence signal was found in other organs (Supplemental Fig. S5). All measurements were normalized to the total flux on d 0 to permit comparisons among individual mice. Figure 4*B* shows representative results for 2 mice and Fig. 3*C* shows the relative flux for all mice (see Supplemental Fig. S6 for a validation experiment with a longer follow-up).

Whereas the growth rates of $NCS1^+$ and control tumors are comparable from d 7 onwards, the biggest difference between the groups can be observed between d 0 and 7. Consistent with our *in vitro* results, these *in vivo* findings suggest that NCS1-OE tumor cells have a survival advantage in the early phase of tumor development (Fig. 4*C*).

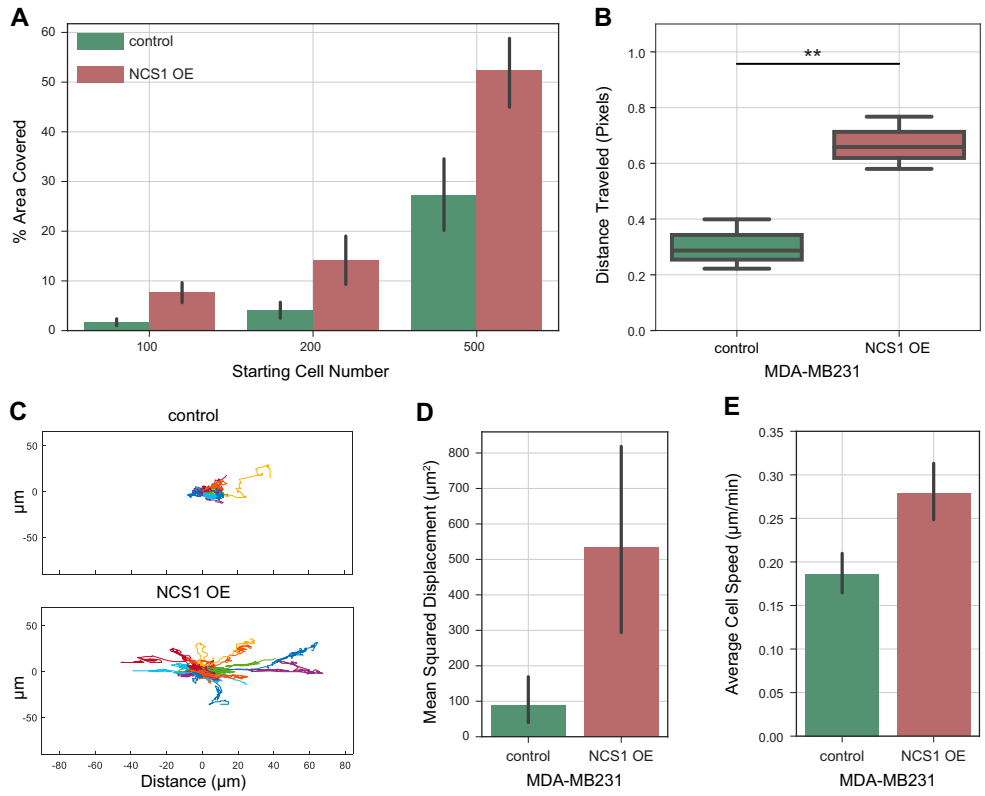

Figure 3. NCS1 overexpression increases cellular motility in 2- and 3-D cell culture experiments. *A*) Bar plot of a colony formation assay with MDA-MB231 control and NCS1-OE cells. The assay was performed with 100, 200, and 500 initial cells, and the plot shows the percentage area covered at the end of the experiment as mean values ± 95% confidence intervals ($P < 0.01$ for all comparisons). *B*) Scratch assay demonstrating the wound healing capacity of NCS1-OE and control MDA-MB231 cells. The distance traveled (in pixels) was assessed after 24 h. Box plots represent $n = 3$ independent experiments per genotype. $^{**}P < 0.01$. *C*) Line plots showing the movement of MDA-MB231 control and NCS1-OE cells in collagen gels over a period of 8 h (in micrometers) as measured using time-lapse microscopy. Each colored trace represents an individual cell. *D, E*) Bar plots showing the MSD (μM^2) (*D*) and average velocity (µM/min) (*E*) of MDA-MB231 control and NCS1-OE cells in collagen gels over a period of 8 h. Values are means of $n = 40$ cells ± 95% confidence intervals ($P < 0.005$ and $P < 0.0001$, respectively).

Histopathologic assessment of lung specimens confirms the presence of multiple tumor cell clusters in the NCS1$^+$ group and small numbers of single tumor cells in the control

During the aforementioned mouse study (**Fig. 5*A***), mouse lungs were harvested after d 3 and 7, and again at the end of the study. Because the biggest differences between NCS1$^+$ and control tumors were found in the early phase (defined as the first 7 d) of tumor development, histopathologic assessment was conducted with a focus on these early tumors.

Lung tissue collected 7 d after tumor cell injection showed only a rare appearance of cancer cells in the lung specimens isolated from control mice and stained with H&E (Fig. 5*A* and Supplemental Table S2). Only 3 of the 8 control mouse lungs were found to contain a few single tumor cells (Supplemental Fig. S7 and Supplemental Table S2), whereas all lungs from NCS1$^+$ mice harbored tumor cells and 6 of these 8 lungs contained multiple clusters of tumor cells (Fig. 5*B, C* and Supplemental Table S2). Anti-NCS1 immunohistochemistry (IHC) staining was used to validate the expression of NCS1 in the cells that were identified as cancer cells in the H&E-stained slides (inset in Fig. 5C and Supplemental Table S3). These results indicate that overexpression of NCS1 causes a higher early incidence of metastasis in mouse lungs after tail-vein injection with a tumor cell suspension. This can be explained by an increase of the number of cells which survived to form colonies in the lung tissue or an increase of cell invasiveness upon NCS1 overexpression.

NCS1 overexpression confers a long-term survival advantage to tumor cells

Mouse lung specimens that were obtained at the end of the study were stained with H&E and inspected to investigate

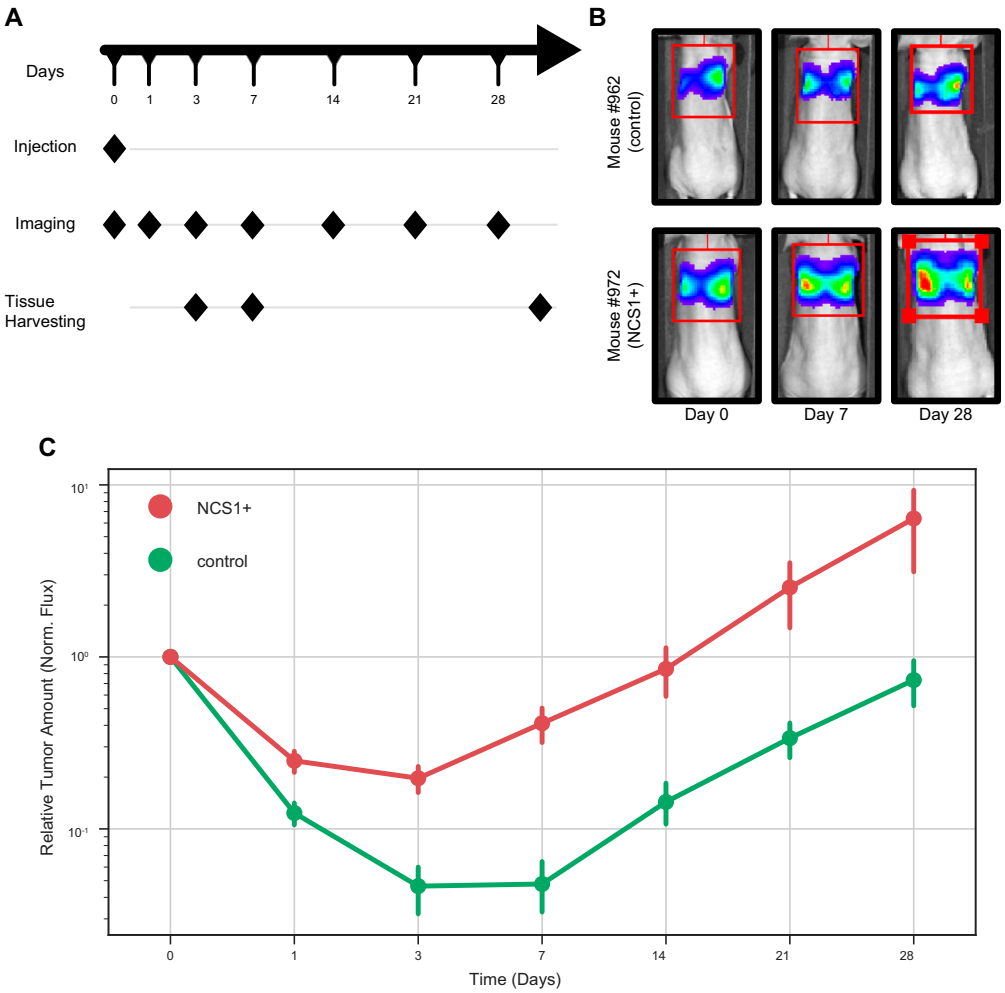

Figure 4. Mouse xenograft experiments show larger lung tumors from NCS1+-containing cells when compared with the control. *A*) Workflow schematic; $n = 16$ mice per group were injected *via* the tail vein with MDA-MB231 breast cancer cells overexpressing either NCS1 or a control vector. Lung tissue of 4 mice per group was harvested after 3 and 7 d and all mice were euthanized at the end of the study after d 28. Imaging studies measuring the photon flux of a luciferase reporter was performed on d 1, 3, 7, 14, 21, and 28. *B*) The panels show representative mouse images of a control mouse (962) and an NCS1$^+$ mouse (972). The color-coded luminescence signal indicates the relative amount of tumor in the mouse lungs with blue being a weak signal and red being a strong signal. *C*) Line plot showing the relative luminescence signal after normalization at each imaging time point. Until d 7, the fluorescence measurements decreased less in NCS1$^+$ tumors (red line plot) than in control tumors (green line plot). All tumors grow at similar rates from d 7 onwards.

the question whether NCS1 plays a role in mature tumors as well. Because all mice were euthanized after the respective lung tumor reached a large, predetermined size (10^9 absolute flux as measured using the method described above), a homogeneous histologic appearance of NCS1$^+$ and control tumors was anticipated.

Contrary to our expectations, we found large areas of necrosis in the control tumors (**Fig. 6*A***), whereas no necrotic cells could be identified in 3 of the 4 specimens from NCS1$^+$ tumors (Fig. 6*B* and Supplemental Table S1). A fourth specimen exhibited limited amounts of necrotic material as opposed to the large areas of necrosis in the control tumors. Histologically, no difference with regard to the overall tumor volume was found between NCS1$^+$ and control lungs, most likely because all tumors had reached a size where the lungs were completely filled with tumor cells (Supplemental Fig. S8). The absence of tumor cell death in the context of NCS1 overexpression suggests that even in a larger tumor, high NCS1 levels confer a survival advantage. This may impact the reactivity of the

tumor to treatment by preserving more living cells in the tumor's core.

DISCUSSION

In this study, we examined the effects of increased levels of NCS1 on tumor cell migration and survival *in vitro* and *in vivo*. We have previously observed that high NCS1 expression was significantly associated with an unfavorable prognosis in 2 independent breast cancer cohorts (41) as well as 2 publicly available liver cancer cohorts (42). Interestingly, NCS1 levels were highly correlated with expression levels of LIMK1, an enzyme associated with regulation of cell motility (27), when examining RNA sequencing data of liver samples from the Cancer Genome Atlas (48) and the International Cancer Genome Consortium (49). LIMK1 is a key regulator of the actin cytoskeleton and its high expression was previously identified as a potential driver of invasion in a variety of tumors (28–30). Other components of physiologic Ca^{2+} signaling are also known to regulate physiologic cell movement as well as tumor cell motility (21, 22, 24). Thus, we hypothesized that high levels of NCS1 may confer enhanced metastatic capability on tumor cells.

To investigate the molecular effects of increased NCS1, this Ca^{2+}-binding protein was stably overexpressed in the MDA-MB231 breast cancer cell line. First, we validated (41) that high levels of NCS1 do not alter cellular proliferation rates using 2 cell based growth assays. Another hallmark of aggressive, metastatic tumor cells shown to be regulated by NCS1 is their motility, which would enhance a cell's ability to spread to distant organs within the body. Accordingly, we found that upon overexpression of NCS1, cells exhibited a profoundly different morphology. In particular, they were less rounded and displayed an increased number of large cellular protrusions. This phenotype is consistent with enhanced motility and the capacity to form colonies.

To further study the effects of NCS1 overexpression on tumor cell morphology, immunofluorescence imaging was performed. We found that NCS1 preferentially localizes to the leading edge of migrating cells. Although this effect was independent of absolute expression levels, we found more NCS1 at cellular protrusions in cells that highly overexpressed NCS1. This finding supports the hypothesis that NCS1 might facilitate the movement of cancer cells *via* regulation of local Ca^{2+} at cell extensions. The colocalization between NCS1 and actin, specifically at the leading edge, suggests that NCS1 assists in regulating the continuous turnover of the actin cytoskeleton necessary for cell migration to occur.

We performed 2-D colony formation and wound healing assays to confirm that this morphologic change is also accompanied by a functional change. Indeed, NCS1-OE cells were more motile compared with the controls. In an attempt to more closely mimic the physiologic 3-D

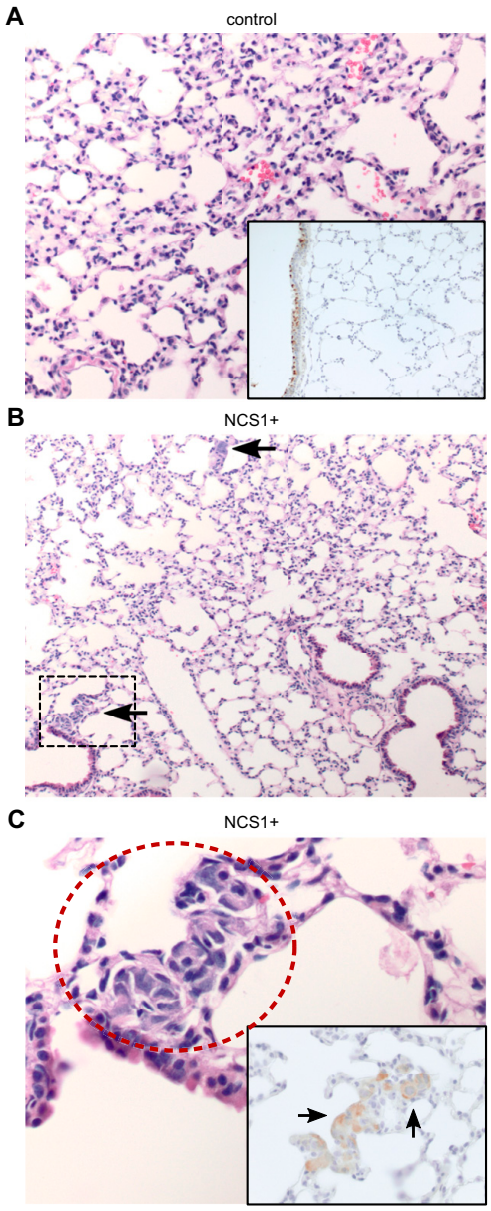

Figure 5. Lung specimens of NCS1+ mice contain large tumor cell clusters after 7 d. *A*) Tumor cells were not found in an H&E-stained lung specimen from a control mouse (966) that was euthanized after 7 d (medium magnification). Anti-NCS1 IHC staining confirms the absence of tumor cells (insert, high magnification). NCS1 staining within normal bronchial epithelium served as a positive control in all samples. *B*) Two prominent foci of tumor cells are visible (black arrows) in an H&E-stained lung specimen from an NCS1+ mouse (987) that was euthanized after 7 d (low magnification). *C*) High-magnification image of the region in *B* that is marked with a black box. Tumor cells are circled in red. The insert shows an anti-NCS1 IHC-stained specimen of mouse 987 (high magnification) demonstrating that the tumor cells were stained positively for NCS1 (black arrows).

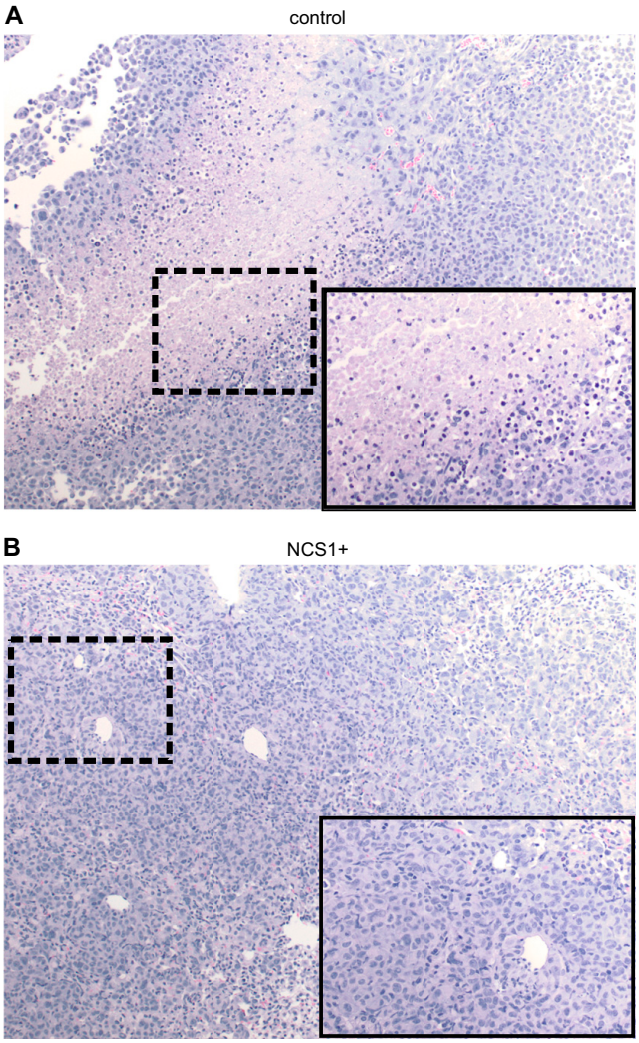

Figure 6. Lung specimens of NCS1^{+} mice show no necrotic areas after more than 28 d of tumor growth. *A*) H&E-stained lung specimen (medium magnification) of a control mouse (952) at the end of the study. The insert shows an area of necrosis (black box) at high magnification. *B*) Picture of an H&E-stained lung specimen (medium magnification) of an NCS1^{+} mouse (973) at the end of the study. Note the absence of necrotic cells. The insert shows a high magnification view of the area in the black box.

microenvironment in which cancers grow and to analyze the dynamics of MDA-MB231 cell movement *in vitro* (50, 51), we placed NCS1-OE and control cells in type I collagen gels and performed time-lapse microscopy to monitor their movement. Again, increased motility, as measured using the MSD and average speed, was observed.

Thus, the *in vitro* experiments performed in this study suggest that tumor cells that acquire high levels of NCS1 during tumorigenesis gain the advantage of being more motile. To explore the question of whether this *in vitro* phenotype also leads to an increased number of metastases *in vivo*, we used a mouse xenograft model. Engineered MDA-MB231 cells were injected into the tail vein of nude mice and a luciferase reporter was used to monitor tumor growth in the mouse lungs over time. Mice injected with high NCS1 levels presented with increased numbers of nascent tumors between d 0 and 7, but after this initial period, the growth rates of NCS1^{+} and control tumors were similar. This finding in an intact mouse is in close alignment with our observations from *in vitro* experiments. If NCS1 impacted cell proliferation, we would have expected to see a difference in the overall tumor growth rates.

That NCS1 facilitates early tumor cell engraftment in the mouse lung suggests that NCS1 promotes cell survival as well as metastasis. In addition to examining mouse specimens at early time points during the experiment, specimens from larger tumors after more than 28 d were analyzed to gain more insight into how NCS1 overexpression impacts tumor behavior. Although all of the tumors were large, we observed differences between the groups. Control tumors presented with large necrotic

zones in all specimens, whereas NCS1$^+$ tumors did not. This difference indicates a survival advantage of cells with high NCS1 levels that extends beyond the initial metastatic expansion.

It is well known that major oncogenic pathways are regulated by cytoplasmic Ca^{2+}. Enhanced signaling *via* the PI3K/Akt pathway facilitates cell movement and increases cellular survival (52). NCS1 physically binds to PI4K (35, 36) and *via* this protein–protein interaction, it regulates the production of the second messenger molecule inositol 1,4,5 *tris*phosphate (53). InsP3 in turn activates the PI3K pathway. Furthermore, NCS1 interacts with InsP3Rs at the endoplasmic reticulum (ER) and upon binding, there is increased Ca^{2+} efflux from the ER (54). Previous research has shown that InsP3Rs are important contributors to an aggressive, prometastatic phenotype in cancer cells (21). The combination of these studies indicates that NCS1 enhances cell migration and survival *via* several routes. Upon overexpression, NCS1 binds to InsP3Rs and increases cytoplasmic Ca^{2+} concentrations. Ca^{2+} itself can act as a second messenger molecule and can facilitate cell movement. In addition, NCS1 may activate the PI3K pathway upon binding to PI4K.

Our previous study used 2 different breast cancer cell lines (MDA-MB231 and MCF-7), and similar responses to NCS1 overexpression were observed in both cell lines (41). In this study we focused on the triple-negative MDA-MB231 cells derived from plural effusion, as these cells are better able to metastasize to various organs (55). Various *in vitro* and *in vivo* experiments were performed to demonstrate the effects of NCS1 overexpression on several aspects of the cellular phenotype. In-depth mechanistic studies of the molecular effects of NCS1 are currently in preparation. Our future work will also reveal which parts of the Ca^{2+} signaling complex associated with NCS1 (42) are best suited for pharmacologic intervention.

CONCLUSIONS

This study demonstrates that overexpression of the Ca^{2+} binding protein NCS1 increases cellular motility and the invasive capacity of tumor cells *in vitro* and *in vivo* without altering growth rates. It lays the groundwork for studying the molecular mechanisms of NCS1- and Ca^{2+}-driven metastasis in cancers such as breast and liver tumors. Furthermore, it describes a set of experiments that can be used to test pharmacologic interventions to inhibit metastatic spread of tumor cells with high levels of NCS1. FJ

ACKNOWLEDGMENTS

The authors thank Dr. Sabine Lang (Yale University) for technical and administrative support. The authors acknowledge helpful discussions with Allison Brill, Dr. David Calderwood, and Dr. Tamar Taddei (Yale University). J.E.A., D.S., J.A.S., and H.K.G. received a scholarship from the German Academic Scholarship Foundation. M.Z. received a Brown Coxe Postdoctoral Fellowship from Yale University. W.L.C. received NSF Graduate Research Fellowship DGE-1122492. This work was supported, in part, by U.S. National Institutes of Health (NIH) National Institute of Diabetes and Digestive and Kidney Diseases Grant 5P01DK057751 (to B.E.E. and M.E.R.), NIH National Institute of Biomedical Imaging and Bioengineering (Grant 1R21EB026630 to M.M.), and U.S. Department of Defense Grant W81XWH-15-1-0117 (to Q.Y.). B.E.E. is a founder of Osmol Therapeutics, a company that is targeting NCS1 for therapeutic purposes. Primary data are maintained in the Ehrlich Laboratory at Yale University. Reagents not commercially available are available from the Ehrlich Laboratory. The authors declare no conflicts of interest.

AUTHOR CONTRIBUTIONS

J. E. Apasu, D. Schuette, and B. E. Ehrlich designed the study; J. E. Apasu, D. Schuette, R. LaRanger, J. A. Steinle, L. D. Nguyen, H. K. Grosshans, M. Zhang, and W. L. Cai contributed to experiments; M. E. Robert provided all pathology assessments; D. Schuette and B. E. Ehrlich wrote the first draft; and all authors edited the manuscript and have consented to publication.

REFERENCES

1. Hanahan, D., and Weinberg, R. A. (2011) Hallmarks of cancer: the next generation. *Cell* **144**, 646–674
2. Mehlen, P., and Puisieux, A. (2006) Metastasis: a question of life or death. *Nat. Rev. Cancer* **6**, 449–458
3. Taketo, M. M. (2011) Reflections on the spread of metastasis to cancer prevention. *Cancer Prev. Res. (Phila.)* **4**, 324–328
4. Lambert, A. W., Pattabiraman, D. R., and Weinberg, R. A. (2017) Emerging biological principles of metastasis. *Cell* **168**, 670–691
5. Berridge, M. J. (1993) Inositol trisphosphate and calcium signalling. *Nature* **361**, 315–325
6. Berridge, M. J. (1998) Neuronal calcium signaling. *Neuron* **21**, 13–26
7. Nguyen, T., Chin, W. C., and Verdugo, P. (1998) Role of Ca^{2+}/K^+ ion exchange in intracellular storage and release of Ca2+. *Nature* **395**, 908–912
8. Gunter, T. E., and Pfeiffer, D. R. (1990) Mechanisms by which mitochondria transport calcium. *Am. J. Physiol.* **258**, C755–C786
9. Berridge, M. J. (1995) Calcium signalling and cell proliferation. *BioEssays* **17**, 491–500
10. Smedler, E., and Uhlén, P. (2014) Frequency decoding of calcium oscillations. *Biochim. Biophys. Acta* **1840**, 964–969
11. Dolmetsch, R. E., Xu, K., and Lewis, R. S. (1998) Calcium oscillations increase the efficiency and specificity of gene expression. *Nature* **392**, 933–936
12. Clapham, D. E. (2007) Calcium signaling. *Cell* **131**, 1047–1058
13. Augustine, G. J., Santamaria, F., and Tanaka, K. (2003) Local calcium signaling in neurons. *Neuron* **40**, 331–346
14. Ghosh, A., and Greenberg, M. E. (1995) Calcium signaling in neurons: molecular mechanisms and cellular consequences. *Science* **268**, 239–247
15. Hajnóczky, G., Davies, E., and Madesh, M. (2003) Calcium signaling and apoptosis. *Biochem. Biophys. Res. Commun.* **304**, 445–454
16. Takemura, M., Mishima, T., Wang, Y., Kasahara, J., Fukunaga, K., Ohashi, K., and Mizuno, K. (2009) Ca^{2+}/calmodulin-dependent protein kinase IV-mediated LIM kinase activation is critical for calcium signal-induced neurite outgrowth. *J. Biol. Chem.* **284**, 28554–28562
17. Hanna, S., and El-Sibai, M. (2013) Signaling networks of Rho GTPases in cell motility. *Cell. Signal.* **25**, 1955–1961
18. Zheng, J. Q., and Poo, M. M. (2007) Calcium signaling in neuronal motility. *Annu. Rev. Cell Dev. Biol.* **23**, 375–404
19. Swaney, K. F., Huang, C.-H., and Devreotes, P. N. (2010) Eukaryotic chemotaxis: a network of signaling pathways controls motility, directional sensing, and polarity. *Annu. Rev. Biophys.* **39**, 265–289
20. Yi, M., Weaver, D., and Hajnóczky, G. (2004) Control of mitochondrial motility and distribution by the calcium signal: a homeostatic circuit. *J. Cell Biol.* **167**, 661–672
21. Ando, H., Kawaai, K., Bonneau, B., and Mikoshiba, K. (2018) Remodeling of Ca^{2+} signaling in cancer: regulation of inositol 1,4,5-trisphosphate receptors through oncogenes and tumor suppressors. *Adv. Biol. Regul.* **68**, 64–76

22. Florea, A. M., and Büsselberg, D. (2009) Anti-cancer drugs interfere with intracellular calcium signaling. *Neurotoxicology* **30**, 803–810
23. Chen, Y. F., Chen, Y. T., Chiu, W. T., and Shen, M. R. (2013) Remodeling of calcium signaling in tumor progression. *J. Biomed. Sci.* **20**, 23
24. Stewart, T. A., Yapa, K. T. D. S., and Monteith, G. R. (2015) Altered calcium signaling in cancer cells. *Biochim. Biophys. Acta* **1848**, 2502–2511
25. Xiao, M., Li, T., Ji, Y., Jiang, F., Ni, W., Zhu, J., Bao, B., Lu, C., and Ni, R. (2018) S100A11 promotes human pancreatic cancer PANC-1 cell proliferation and is involved in the PI3K/AKT signaling pathway. *Oncol. Lett.* **15**, 175–182
26. Gonzalez Guerrico, A. M., Jaffer, Z. M., Page, R. E., Braunewell, K. H., Chernoff, J., and Klein-Szanto, A. J. (2005) Visinin-like protein-1 is a potent inhibitor of cell adhesion and migration in squamous carcinoma cells. *Oncogene* **24**, 2307–2316
27. Prunier, C., Prudent, R., Kapur, R., Sadoul, K., and Lafanechère, L. (2017) LIM kinases: cofilin and beyond. *Oncotarget* **8**, 41749–41763
28. Scott, R. W., Hooper, S., Crighton, D., Li, A., Kõnig, I., Munro, J., Trivier, E., Wickman, G., Morin, P., Croft, D. R., Dawson, J., Machesky, L., Anderson, K. I., Sahai, E. A., and Olson, M. F. (2010) LIM kinases are required for invasive path generation by tumor and tumor-associated stromal cells. *J. Cell Biol.* **191**, 169–185
29. Scott, R. W., and Olson, M. F. (2007) LIM kinases: function, regulation and association with human disease. *J. Mol. Med. (Berl.)* **85**, 555–568
30. Li, R., Doherty, J., Antonipillai, J., Chen, S., Devlin, M., Visser, K., Baell, J., Street, I., Anderson, R. L., and Bernard, O. (2013) LIM kinase inhibition reduces breast cancer growth and invasiveness but systemic inhibition does not reduce metastasis in mice. *Clin. Exp. Metastasis* **30**, 483–495
31. Boeckel, G. R., and Ehrlich, B. E. (2018) NCS-1 is a regulator of calcium signaling in health and disease. *Biochim. Biophys. Acta. Mol. Cell Res.* **1865**, 1660–1667
32. Weiss, J. L., Hui, H., and Burgoyne, R. D. (2010) Neuronal calcium sensor-1 regulation of calcium channels, secretion, and neuronal outgrowth. *Cell. Mol. Neurobiol.* **30**, 1283–1292
33. D'Onofrio, S., Kezunovic, N., Hyde, J. R., Luster, B., Messias, E., Urbano, F. J., and Garcia-Rill, E. (2015) Modulation of gamma oscillations in the pedunculopontine nucleus by neuronal calcium sensor protein-1: relevance to schizophrenia and bipolar disorder. *J. Neurophysiol.* **113**, 709–719
34. Burgoyne, R. D., and Weiss, J. L. (2001) The neuronal calcium sensor family of Ca^{2+}-binding proteins. *Biochem. J.* **353**, 1–12
35. Rajebhosale, M., Greenwood, S., Vidugiriene, J., Jeromin, A., and Hilfiker, S. (2003) Phosphatidylinositol 4-OH kinase is a downstream target of neuronal calcium sensor-1 in enhancing exocytosis in neuroendocrine cells. *J. Biol. Chem.* **278**, 6075–6084
36. Haynes, L. P., Fitzgerald, D. J., Wareing, B., O'Callaghan, D. W., Morgan, A., and Burgoyne, R. D. (2006) Analysis of the interacting partners of the neuronal calcium-binding proteins L-CaBP1, hippocalcin, NCS-1 and neurocalcin δ. *Proteomics* **6**, 1822–1832
37. Blasiole, B., Kabbani, N., Boehmler, W., Thisse, B., Thisse, C., Canfield, V., and Levenson, R. (2005) Neuronal calcium sensor-1 gene ncs-1a is essential for semicircular canal formation in zebrafish inner ear. *J. Neurobiol.* **64**, 285–297
38. Koizumi, S., Rosa, P., Willars, G. B., Challiss, R. A., Taverna, E., Francolini, M., Bootman, M. D., Lipp, P., Inoue, K., Roder, J., and Jeromin, A. (2002) Mechanisms underlying the neuronal calcium sensor-1–evoked enhancement of exocytosis in PC12 cells. *J. Biol. Chem.* **277**, 30315–30324
39. Choe, C. U., and Ehrlich, B. E. (2006) The inositol 1,4,5-trisphosphate receptor (IP3R) and its regulators: sometimes good and sometimes bad teamwork. *Sci. STKE* **2006**, re15
40. Boehmerle, W., Splittgerber, U., Lazarus, M. B., McKenzie, K. M., Johnston, D. G., Austin, D. J., and Ehrlich, B. E. (2006) Paclitaxel induces calcium oscillations via an inositol 1,4,5-trisphosphate receptor and neuronal calcium sensor 1-dependent mechanism. *Proc. Natl. Acad. Sci. USA* **103**, 18356–18361
41. Moore, L. M., England, A., Ehrlich, B. E., and Rimm, D. L. (2017) Calcium sensor, NCS-1, promotes tumor aggressiveness and predicts patient survival. *Mol. Cancer Res.* **15**, 942–952
42. Schuette, D., Moore, L. M., Robert, M. E., Taddei, T. H., and Ehrlich, B. E. (2018) Hepatocellular carcinoma outcome is predicted by expression of neuronal calcium sensor 1. *Cancer Epidemiol. Biomarkers Prev.* **27**, 1091–1100
43. Guzmán, C., Bagga, M., Kaur, A., Westermarck, J., and Abankwa, D. (2014) ColonyArea: an ImageJ plugin to automatically quantify colony formation in clonogenic assays. *PLoS One* **9**, e92444
44. Livak, K. J., and Schmittgen, T. D. (2001) Analysis of relative gene expression data using real-time quantitative PCR and the $2^{-\Delta\Delta C_T}$ method. *Methods* **25**, 402–408
45. Ponomarev, V., Doubrovin, M., Serganova, I., Vider, J., Shavrin, A., Beresten, T., Ivanova, A., Ageyeva, L., Tourkova, V., Balatoni, J., Bornmann, W., Blasberg, R., and Gelovani Tjuvajev, J. (2004) A novel triple-modality reporter gene for whole-body fluorescent, bioluminescent, and nuclear noninvasive imaging. *Eur. J. Nucl. Med. Mol. Imaging.* **31**, 740–751
46. Stuelten, C. H., Parent, C. A., and Montell, D. J. (2018) Cell motility in cancer invasion and metastasis: insights from simple model organisms. *Nat. Rev. Cancer* **18**, 296–312
47. Friedl, P., and Gilmour, D. (2009) Collective cell migration in morphogenesis, regeneration and cancer. *Nat. Rev. Mol. Cell Biol.* **10**, 445–457
48. Cancer Genome Atlas Research Network. (2017) Comprehensive and integrative genomic characterization of hepatocellular carcinoma. *Cell* **169**, 1327–1341.e23
49. Fujimoto, A., Furuta, M., Totoki, Y., Tsunoda, T., Kato, M., Shiraishi, Y., Tanaka, H., Taniguchi, H., Kawakami, Y., Ueno, M., Gotoh, K., Ariizumi, S., Wardell, C. P., Hayami, S., Nakamura, T., Aikata, H., Arihiro, K., Boroevich, K. A., Abe, T., Nakano, K., Maejima, K., Sasaki-Oku, A., Ohsawa, A., Shibuya, T., Nakamura, H., Hama, N., Hosoda, F., Arai, Y., Ohashi, S., Urushidate, T., Nagae, G., Yamamoto, S., Ueda, H., Tatsuno, K., Ojima, H., Hiraoka, N., Okusaka, T., Kubo, M., Marubashi, S., Yamada, T., Hirano, S., Yamamoto, M., Ohdan, H., Shimada, K., Ishikawa, O., Yamaue, H., Chayama, K., Miyano, S., Aburatani, H., Shibata, T., and Nakagawa, H. (2016) Whole-genome mutational landscape and characterization of noncoding and structural mutations in liver cancer. *Nat. Genet.* **48**, 500–509
50. Riching, K. M., Cox, B. L., Salick, M. R., Pehlke, C., Riching, A. S., Ponik, S. M., Bass, B. R., Crone, W. C., Jiang, Y., Weaver, A. M., Eliceiri, K. W., and Keely, P. J. (2014) 3D collagen alignment limits protrusions to enhance breast cancer cell persistence. *Biophys. J.* **107**, 2546–2558
51. Wu, P.-H., Giri, A., Sun, S. X., and Wirtz, D. (2014) Three-dimensional cell migration does not follow a random walk. *Proc. Natl. Acad. Sci. USA* **111**, 3949–3954
52. Vivanco, I., and Sawyers, C. L. (2002) The phosphatidylinositol 3-kinase AKT pathway in human cancer. *Nat. Rev. Cancer* **2**, 489–501
53. Balla, A., and Balla, T. (2006) Phosphatidylinositol 4-kinases: old enzymes with emerging functions. *Trends Cell Biol.* **16**, 351–361
54. Schlecker, C., Boehmerle, W., Jeromin, A., DeGray, B., Varshney, A., Sharma, Y., Szigeti-Buck, K., and Ehrlich, B. E. (2006) Neuronal calcium sensor-1 enhancement of InsP3 receptor activity is inhibited by therapeutic levels of lithium. *J. Clin. Invest.* **116**, 1668–1674
55. Fantozzi, A., and Christofori, G. (2006) Mouse models of breast cancer metastasis. *Breast Cancer Res.* **8**, 212

Received for publication September 18, 2018.
Accepted for publication December 3, 2018.

3. Acknowledgments

My thanks go to Prof. Dr. Ehrlich, who has been very supportive during many long hours in the laboratory and who always had valuable advice concerning my experiments as well as the interpretation of their results. Furthermore, I am very grateful to my lab-mates. Without their dedicated training and help with my experiments, as well as their shared thoughts and constructive criticism during many lab-meetings and discussions, the publication, that laid the ground-stone for this dissertation, would not have been possible.

I am also thankful to PD Dr. Jabs, who has helped me with my dissertation in Germany and to the German Academic Scholarship Foundation, that has been supporting me throughout my studies and especially during my research year.

My deepest gratitude goes to my siblings Robert and Giulia, as well as to my parents and friends, who are constantly supporting me and offer me a source of stability and strength not only in academia, but in life in general.